Arrokoth – Orbital Evolution to Contact Binary

Wladimir Lyra

New Mexico State University

Plus:

Andrew Youdin

Anders Johansen

Ringberg Castle - Dec 19th, 2024

Icarus 356 (2021) 113831

Contents lists available at ScienceDirect

Icarus

journal homepage: www.elsevier.com/locate/icarus

Evolution of MU69 from a binary planetesimal into contact by Kozai-Lidov oscillations and nebular drag

W. Lyra[a,*], A.N. Youdin[b], A. Johansen[c]

[a] Department of Astronomy, New Mexico State University, PO BOX 30001, MSC 4500, Las Cruces, NM 88003-8001, United States of America
[b] Steward Observatory, University of Arizona, Tucson, AZ 85721, United States of America
[c] Lund Observatory, Department of Astronomy and Theoretical Physics, Lund University, Box 43, 221 00 Lund, Sweden

ARTICLE INFO

Keywords:
Kuiper belt
Planetesimals
Origin, solar system
Planetary formation

ABSTRACT

The New Horizons flyby of the cold classical Kuiper Belt object MU69 showed it to be a contact binary. The existence of other contact binaries in the 1–10 km range raises the question of how common these bodies are and how they evolved into contact. Here we consider that the pre-contact lobes of MU69 formed as a binary embedded in the Solar nebula, and calculate its subsequent orbital evolution in the presence of gas drag. We find that the sub-Keplerian wind of the disk brings the drag timescales for 10 km bodies to under 1 Myr for quadratic-velocity drag, which is valid in the asteroid belt. In the Kuiper belt, however, the drag is linear with velocity and the effect of the wind cancels out as the angular momentum gained in half an orbit is exactly lost in the other half; the drag timescales for 10 km bodies remain $\gtrsim$10 Myr. In this situation we find that a combination of nebular drag and Kozai-Lidov oscillations is a promising channel for collapse. We analytically solve the hierarchical three-body problem with nebular drag and implement it into a Kozai cycles plus tidal friction model. The permanent quadrupoles of the pre-merger lobes make the Kozai oscillations stochastic, and we find that when gas drag is included the shrinking of the semimajor axis more easily allows the stochastic fluctuations to bring the system into contact. Evolution to contact happens very rapidly (within 10^4 yr) in the pure, double-average quadrupole, Kozai region between $\approx$85 – 95°, and within 3 Myr in the drag-assisted region beyond it. The synergy between J_2 and gas drag widens the window of contact to 80° – 100° initial inclination, over a larger range of semimajor axes than Kozai and J_2 alone. As such, the model predicts a low initial occurrence of binaries in the asteroid belt, and an initial contact binary fraction of about 10% for the cold classicals in the Kuiper belt. The speed at contact is the orbital velocity; if contact happens at pericenter at high eccentricity, it deviates from the escape velocity only because of the oblateness, independently of the semimajor axis. For MU69, the oblateness leads to a 30% decrease in contact velocity with respect to the escape velocity, the latter scaling wi the square root of the density. For mean densities in the range 0.3–0.5 g cm^{-3}, the contact velocity should b – 4.2 m s^{-1}, in line with the observational evidence from the lack of deformation features and estim tensile strength.

1. Introduction

On Jan 1st 2019 the New Horizons spacecraft flew past 2014 MU69 (hereafter referred to as MU69), a small ($\approx$30 km) trans-Neptunian object, recently renamed “Arrokoth”. Its low-eccentricity and low-inclination orbit identifies it as a “cold classical” Kuiper Belt object (CCKBO, Brown, 2001; Kavelaars et al., 2008; Petit et al., 2011). Unlike the heavily processed comet 67P/Churyumov-Gerasimenko visited by the Rosetta mission, MU69 is presumably a pristine planetesimal kept undisturbed for the entirety of its 4.6 Gyr residence in the Kuiper belt.

The flyby showed MU69 to be a contact binary where the two lobes have dimensions 20.6 × 19.9 × 9.4 km and 15.4 × 13.8 × 9.8 km (±0.5×0.5×2, Stern et al., 2019). Their similar colors and composition, as well as axial alignment indicate that the individual lobes formed close to one another, and underwent orbital evolution that led to contact. The close formation is backed by observational data suggesting a high binary fraction among CCKBOs (30%, and possibly larger due to observational limitation, Noll et al., 2008a; Veillet et al., 2002; Petit et al., 2008; Grundy et al., 2011; Fraser et al., 2017). Nearly equal-sized contact binaries represent 10%–25% of cold classicals (Thirouin and Sheppard,

* Corresponding author.
E-mail address: wlyra@nmsu.edu (W. Lyra).

https://doi.org/10.1016/j.icarus.2020.113831
Received 31 October 2019; Received in revised form 20 April 2020; Accepted 27 April 2020
Available online 22 May 2020

Icarus 356 (2021) 113831

Publication: Icarus, Volume 356, article id. 113831.

Pub Date: March 2021

Received 31 October 2019; Received in revised form 20 April 2020; Accepted 27 April 2020

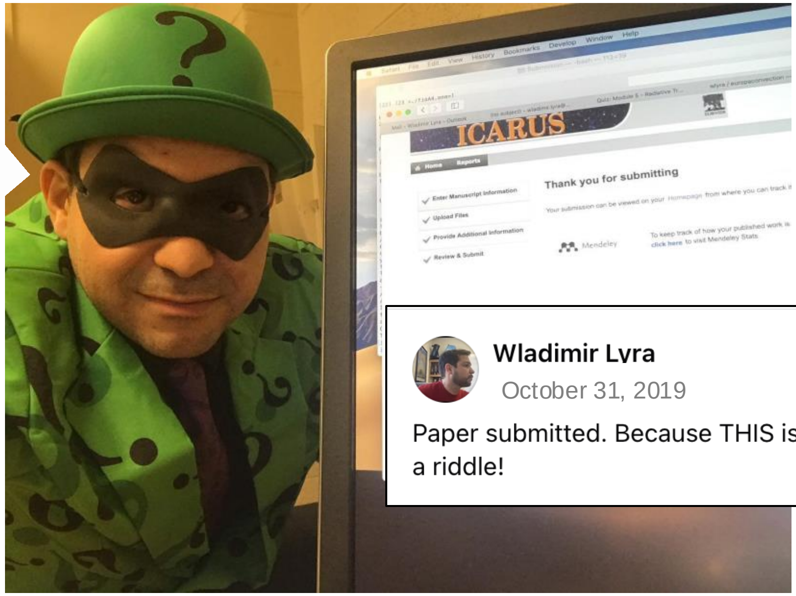

Wladimir Lyra
October 31, 2019

Paper submitted. Because THIS is how to solve a riddle!

I'm afraid that I don't see a Nature paper in this. It's fairly generic and obvious, and as we didn't publish any of the original MU69 papers, there's not an obvious connection. I'm rather skeptical that Nature Astronomy would be interested.

Science
Current Issue First release papers Archive About Submit man
HOME > SCIENCE > VOL. 367, NO. 6481 > THE SOLAR NEBULA ORIGIN OF (486958) ARROKOTH, A PRIMORDIAL CONTACT BINARY IN THE KUIPER BELT
RESEARCH ARTICLE

The solar nebula origin of (486958) Arrokoth, a primordial contact binary in the Kuiper Belt

W. B. MCKINNON, D. C. RICHARDSON, J. C. MAROHNIC, J. T. KEANE, W. M. GRUNDY, D. P. HAMILTON, D. NESVORNÝ, O. M. UMURHAN, T. R. LAUER, [...], AND THE NEW HORIZONS SCIENCE TEAM +19 authors Authors Info & Affiliations

SCIENCE • 13 Feb 2020 • Vol 367, Issue 6481 • DOI: 10.1126/science.aay6620

nature
Explore content About the journal Publish with us
nature > articles > article
Article | Published: 22 April 2020

The wide-binary origin of (2014) MU_{69}-like Kuiper belt contact binaries

Evgeni Grishin, Uri Malamud, Hagai B. Perets, Oliver Wandel & Christoph M. Schäfer

Nature 580, 463–466 (2020) | Cite this article

Icarus 356 (2021) 113831
Contents lists available at ScienceDirect
Icarus
journal homepage: www.elsevier.com/locate/icarus
ELSEVIER

Evolution of MU69 from a binary planetesimal into contact by Kozai-Lidov oscillations and nebular drag

W. Lyra [a,*], A.N. Youdin [b], A. Johansen [c]

[a] Department of Astronomy, New Mexico State University, PO BOX 30001, MSC 4500, Las Cruces, NM 88003-8001, United States of America
[b] Steward Observatory, University of Arizona, Tucson, AZ 85721, United States of America
[c] Lund Observatory, Department of Astronomy and Theoretical Physics, Lund University, Box 43, 221 00 Lund, Sweden

McKinnon et al. (2020) | Grishin et al. (2020) | Lyra et al. (2021)

The Cartoon Image

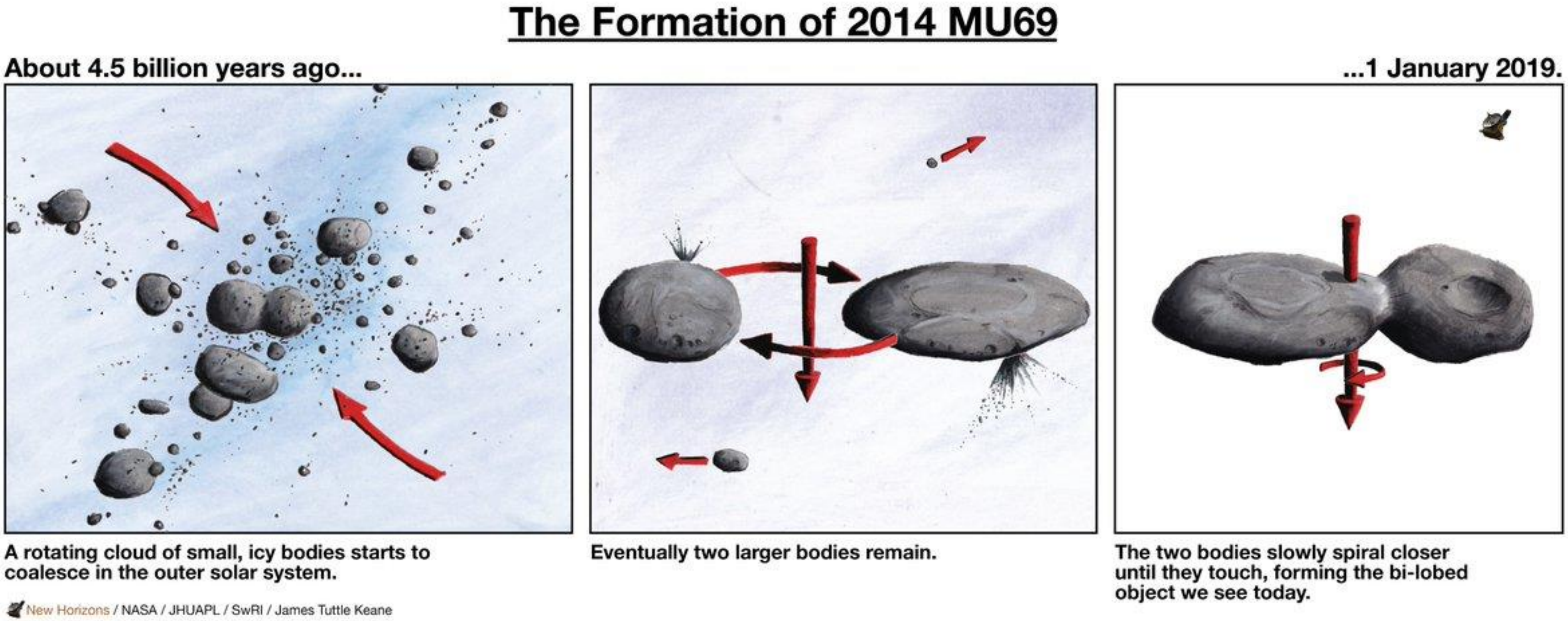

Sketch by J.T. Keane

Arrokoth and Pluto ices are different

Arrokoth : Methanol, H_2O, HCN

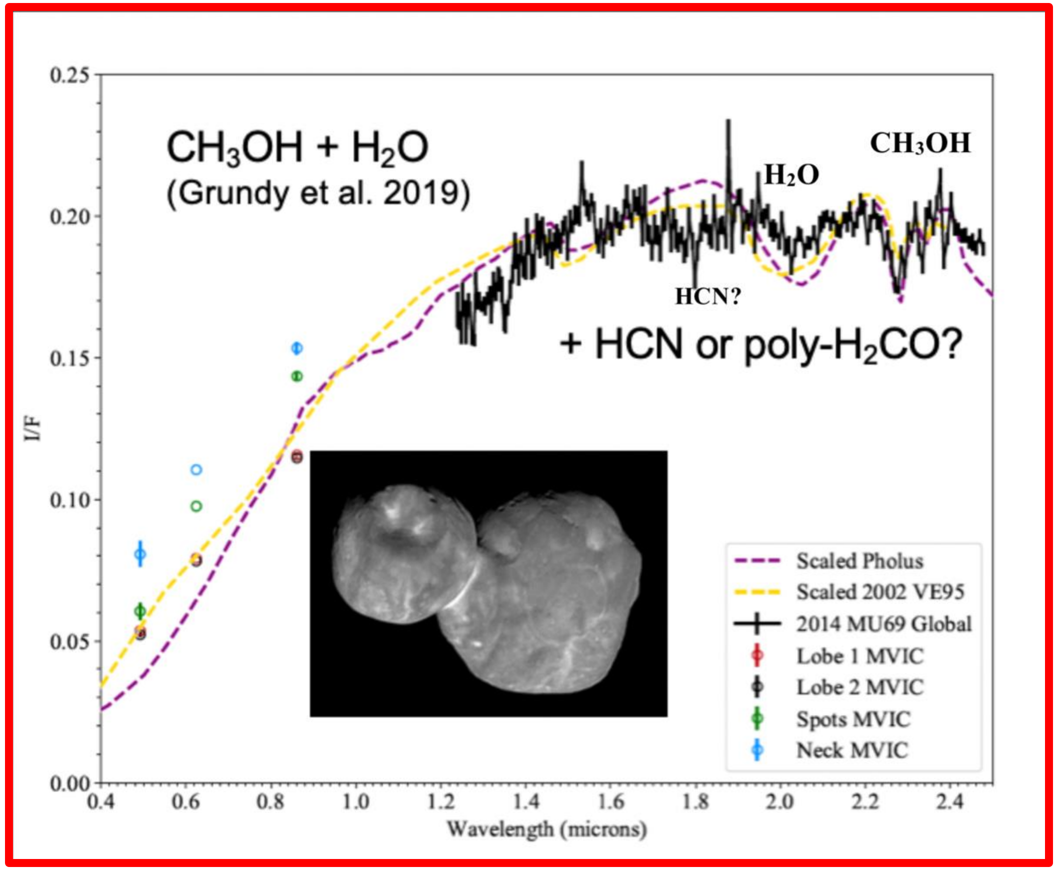

Pluto : CH_4, N_2, CO

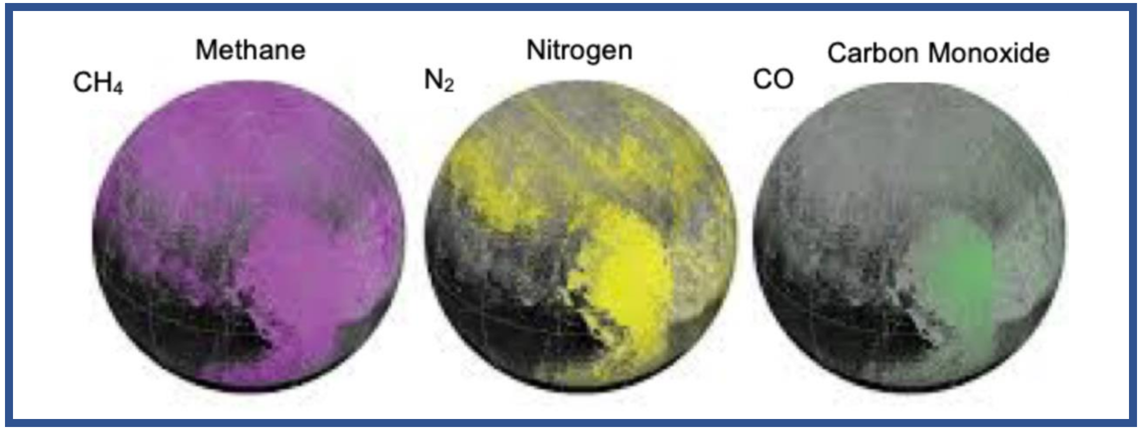

Grundy et al. (2016), Lisse et al. (2020)

Retention of volatiles

If Pluto is formed from similar bodies to Arrokoth, they must retain volatiles

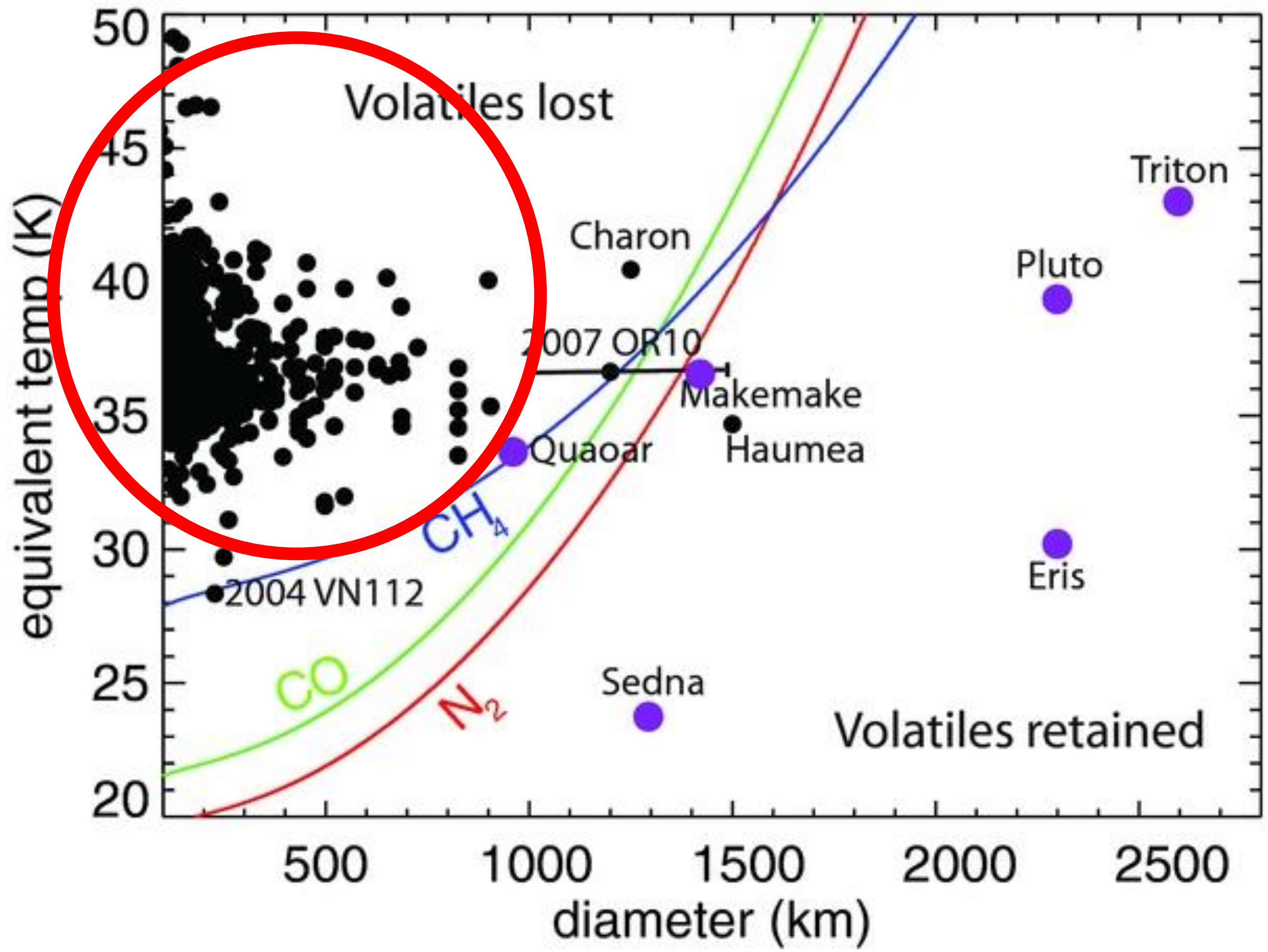

Needs shielding from sunlight

Brown et al. (2011), Lisse et al. (2020)

Retention of volatiles

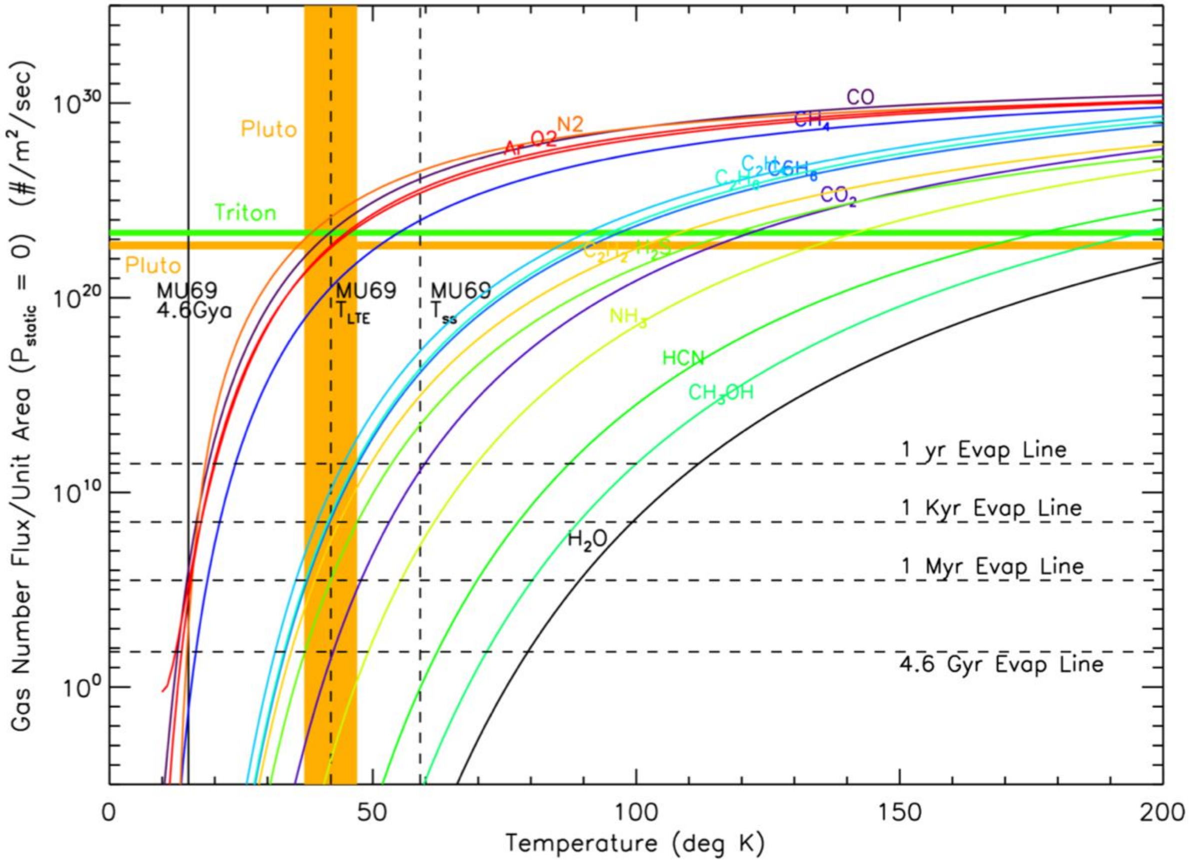

Lisse et al. (2020)

Hypervolatiles (CH_4 / CO / N_2)
lost under vacuum pressure and microgravity in ~1 Myr for 40 K

Retained for long times if formed < 20K

Formation of Arrokoth in an optically thick disk keeps the interior cold enough to allow the volatiles to remain frozen.

Formation via Streaming Instability

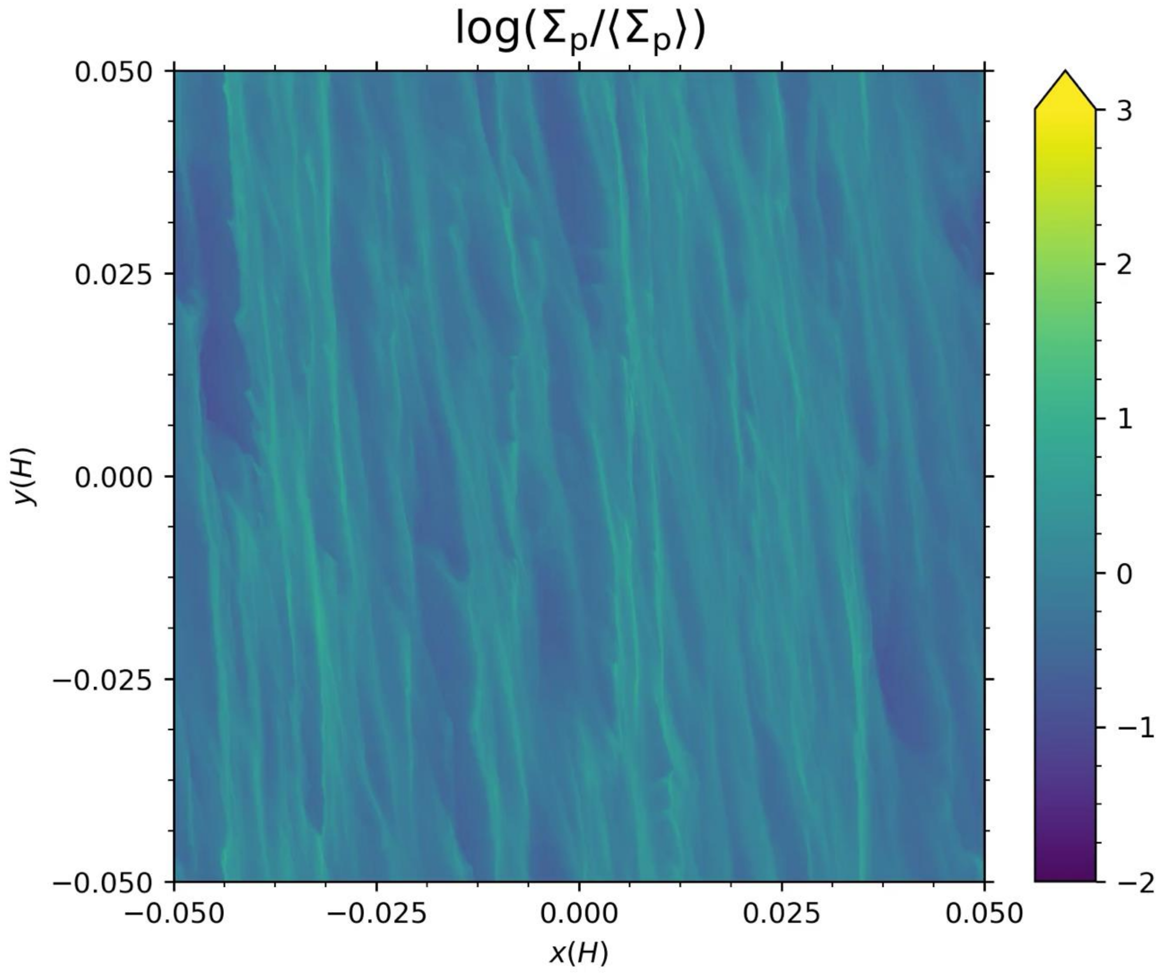

SI Model (solid)
KBOs (dashed)

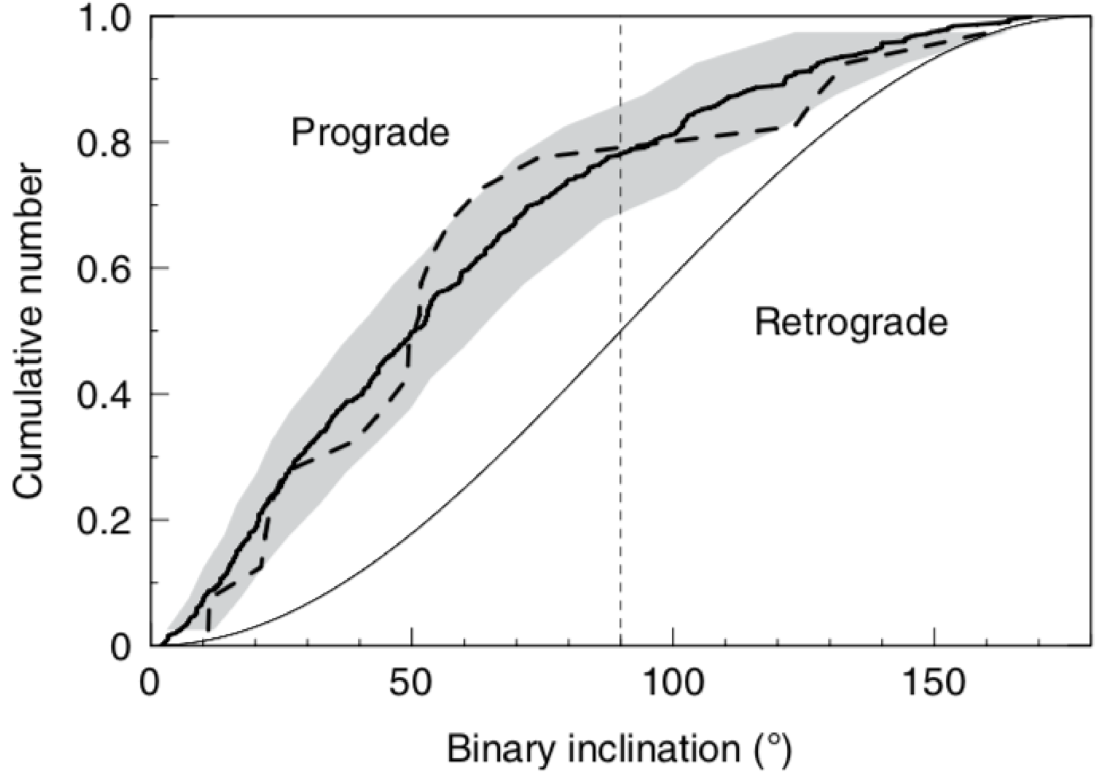

Nesvorny et al. (2019), model by Rixin Li

Hardening

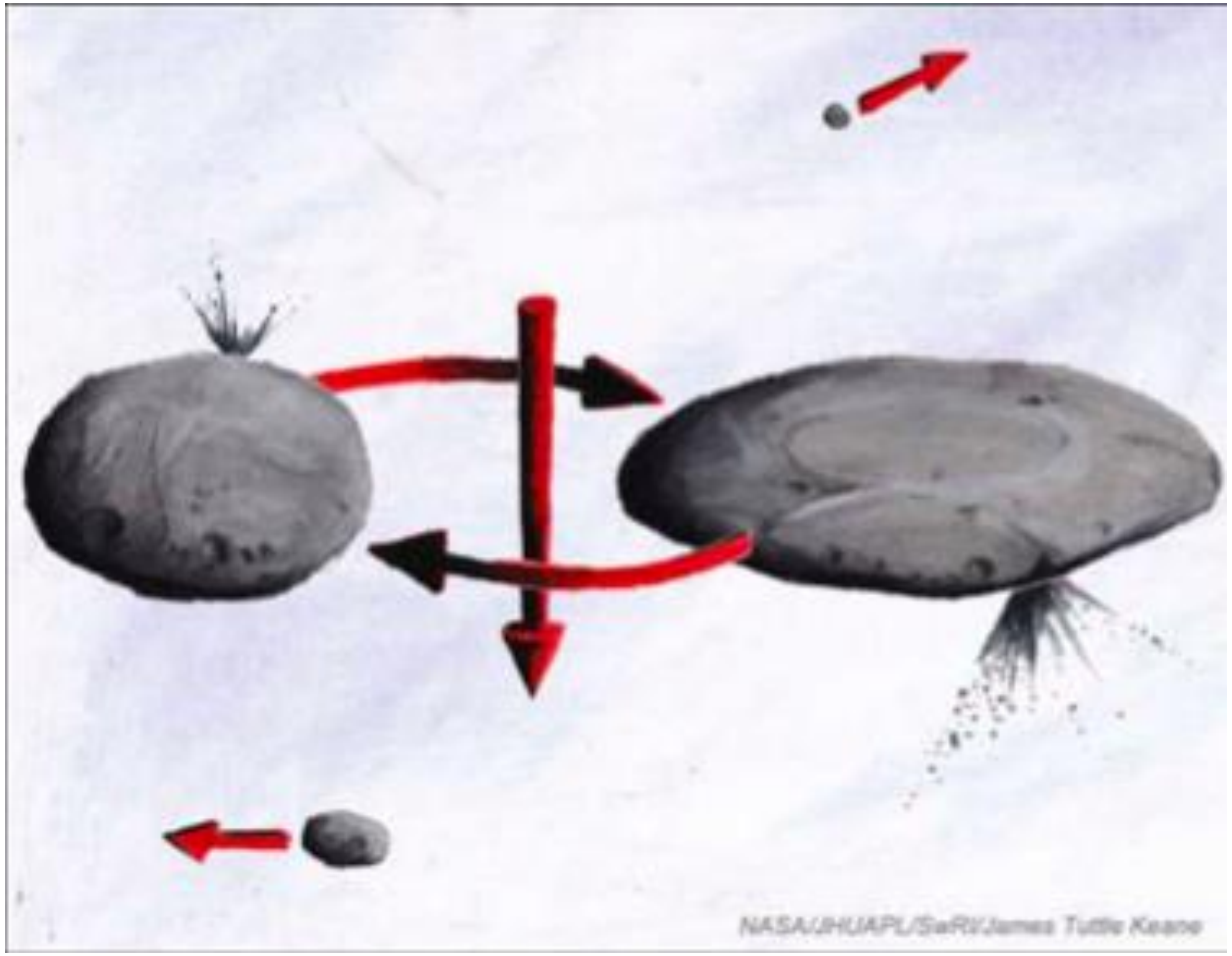

W. Lyra

Sketch by J.T. Keane

How was angular momentum lost?

Before

Mutual orbit
(i.e., not captured)

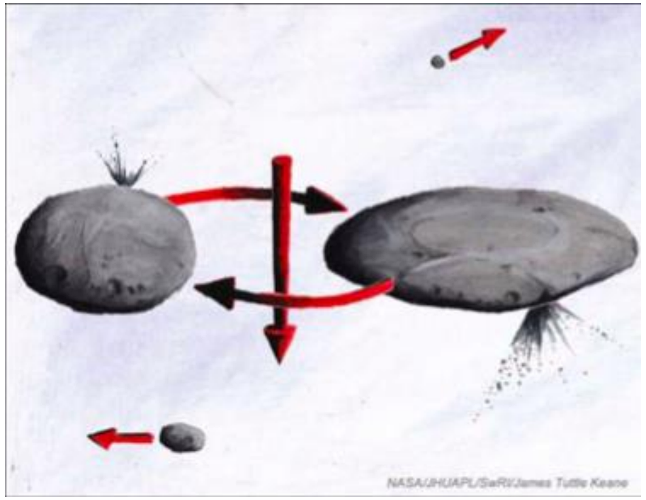

Inferred from:
alignment of component minor axes,
small angular momentum,
similar colors.

After

Slow merger
(~2 m/s: human walking speed)

Inferred from:
Negligible evidence for impact damage

Angular momentum loss via nebular drag

gravity *drag*

$$\ddot{\boldsymbol{r}}_1 = -Gm_2 \frac{(\boldsymbol{r}_1 - \boldsymbol{r}_2)}{|\boldsymbol{r}_1 - \boldsymbol{r}_2|^3} - \frac{\dot{\boldsymbol{r}}_1}{\tau_1}$$

$$\ddot{\boldsymbol{r}}_2 = -Gm_1 \frac{(\boldsymbol{r}_2 - \boldsymbol{r}_1)}{|\boldsymbol{r}_1 - \boldsymbol{r}_2|^3} - \frac{\dot{\boldsymbol{r}}_2}{\tau_2}$$

For equal mass:

$$r\ddot{\phi} + 2\dot{r}\dot{\phi} = -\frac{r\dot{\phi}}{\tau}$$

$$\frac{dh}{dt} = -\frac{h}{\tau}$$

Exponential decay of angular momentum !

$$\boxed{h = h_0 e^{-t/\tau}}$$

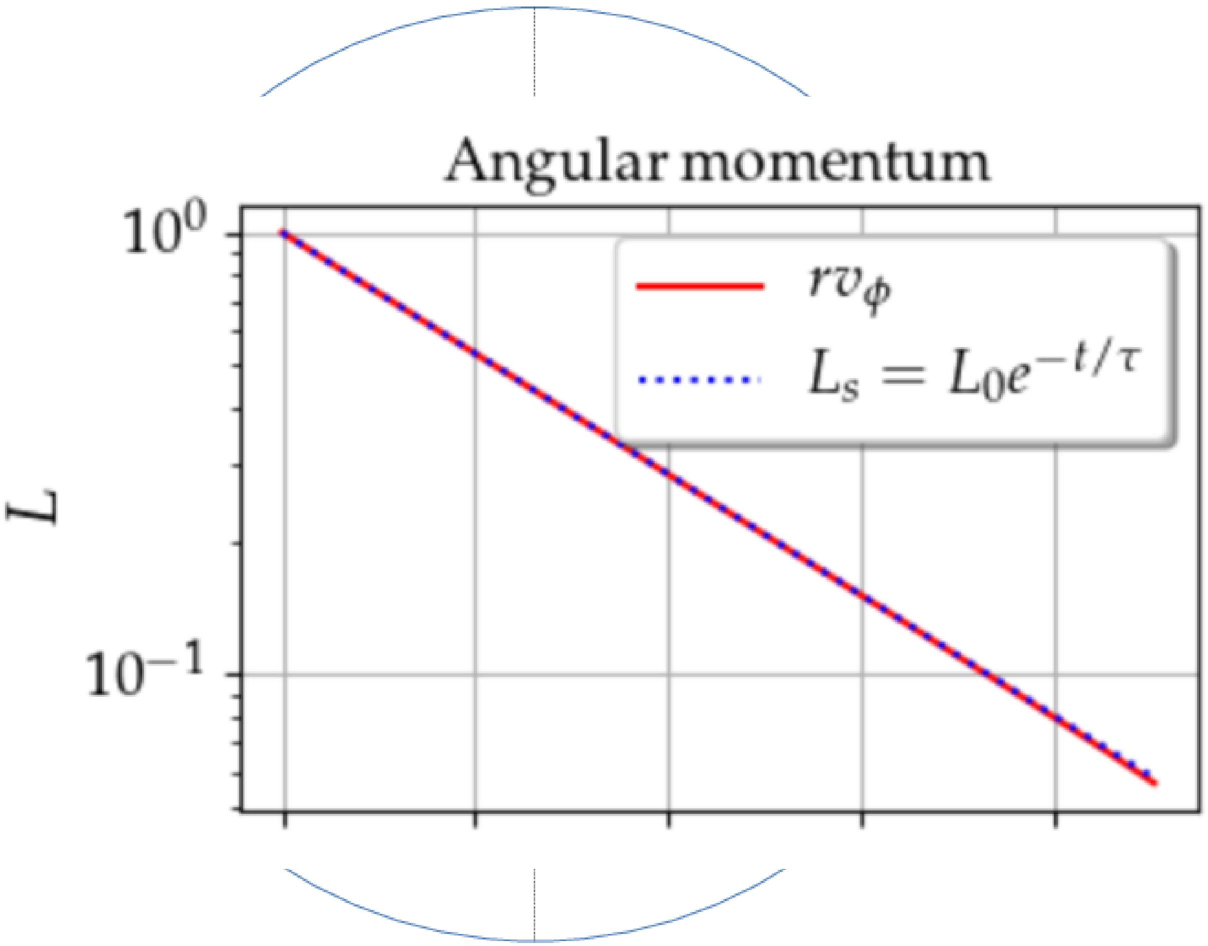

ne

W. Lyra

Lyra, Youdin, & Johansen (2021)

Hardening during disk lifetime

For unequal mass the physics is similar, the
drag time is just replaced by an effective drag time:

Effective drag time

$$\boxed{\tau_{\rm eff} = (m_1 + m_2)\frac{\tau_1\tau_2}{\tau_2 m_2 + \tau_1 m_1}.}$$

Exponential decay of angular momentum

$$\boxed{h = h_0 e^{-t/\tau_{\rm eff}}.}$$

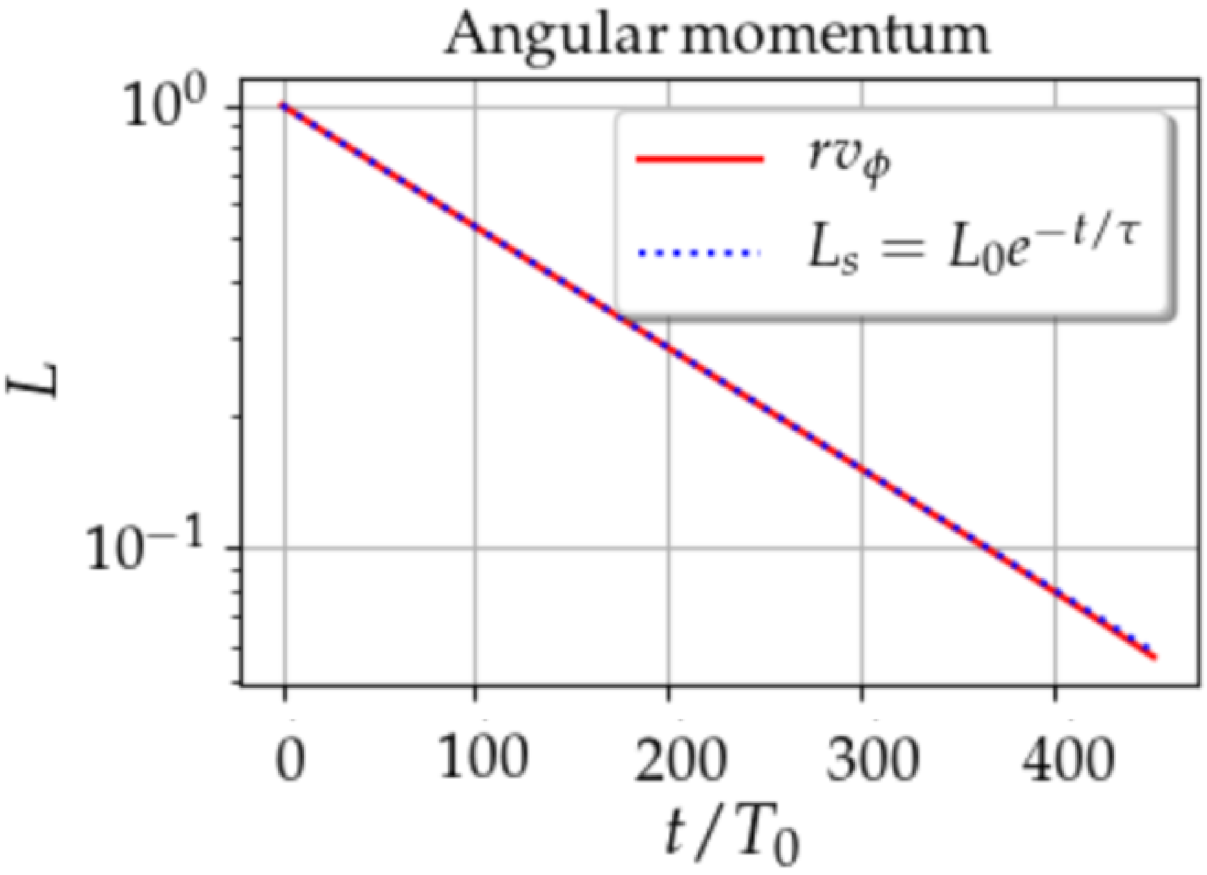

Lyra, Youdin, & Johansen (2021)

Analytical solution

Exponential decay of angular momentum

$$\boxed{h = h_0 e^{-t/\tau_{\rm eff}}}$$

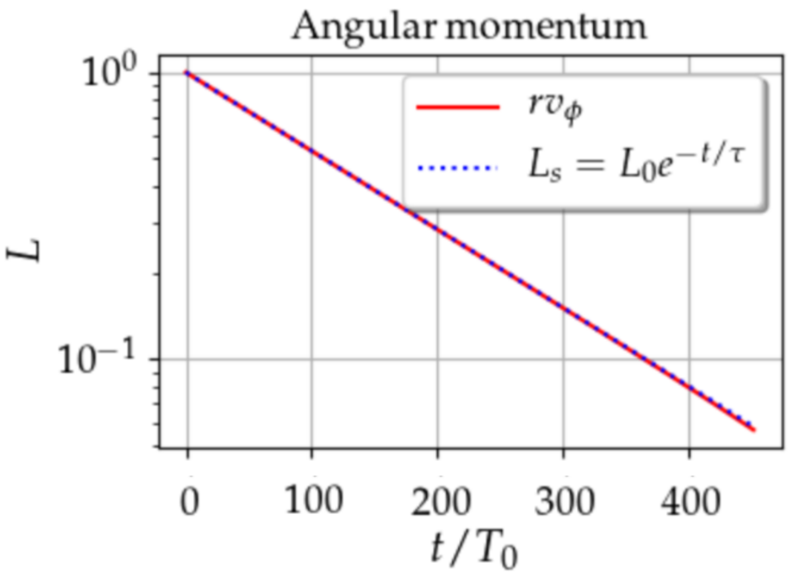

Exponential decay of semimajor axis

$$\boxed{a = a_0\, e^{-2t/\tau_{\rm eff}}}$$

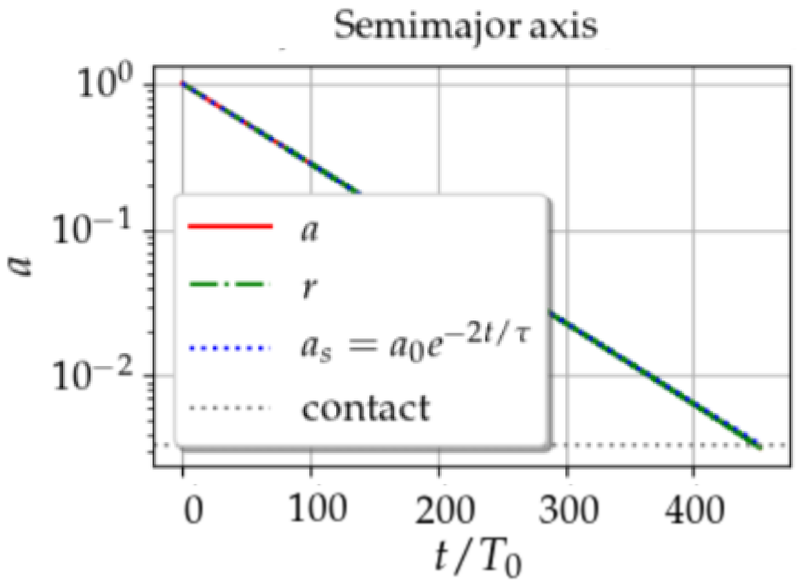

Exponential increase of orbital velocity

$$\boxed{v_\phi = v_{\phi,0}\, e^{t/\tau_{\rm eff}}}$$

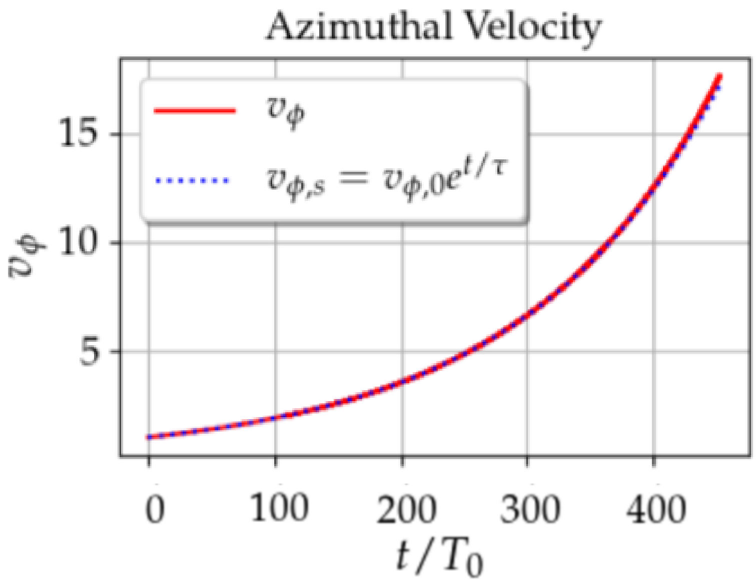

W. Lyra

Lyra, Youdin, & Johansen (2021)

Analytical solution

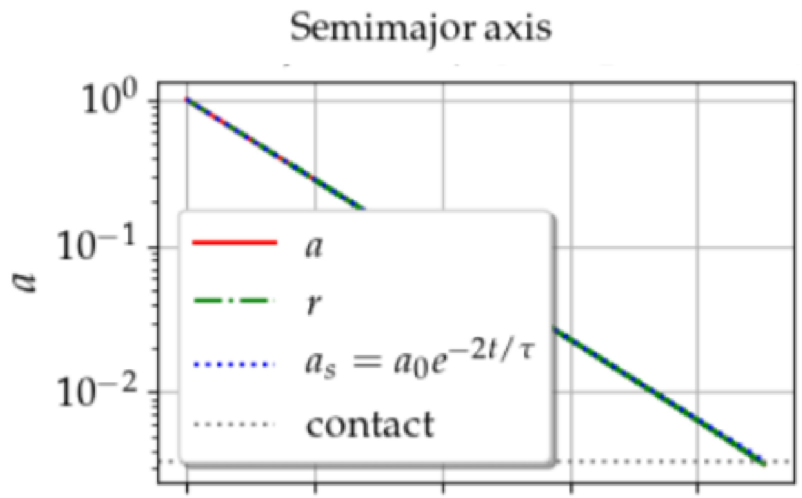

Time until contact

$$t = \frac{\tau}{2} \ln \frac{a_0}{a}$$

For a = *0.1* r_H (6000 km), hardening to a_0=20km and $\tau\Omega=10^7$ …

t ~ 100 Myr

Lyra, Youdin, & Johansen (2021)

Wind

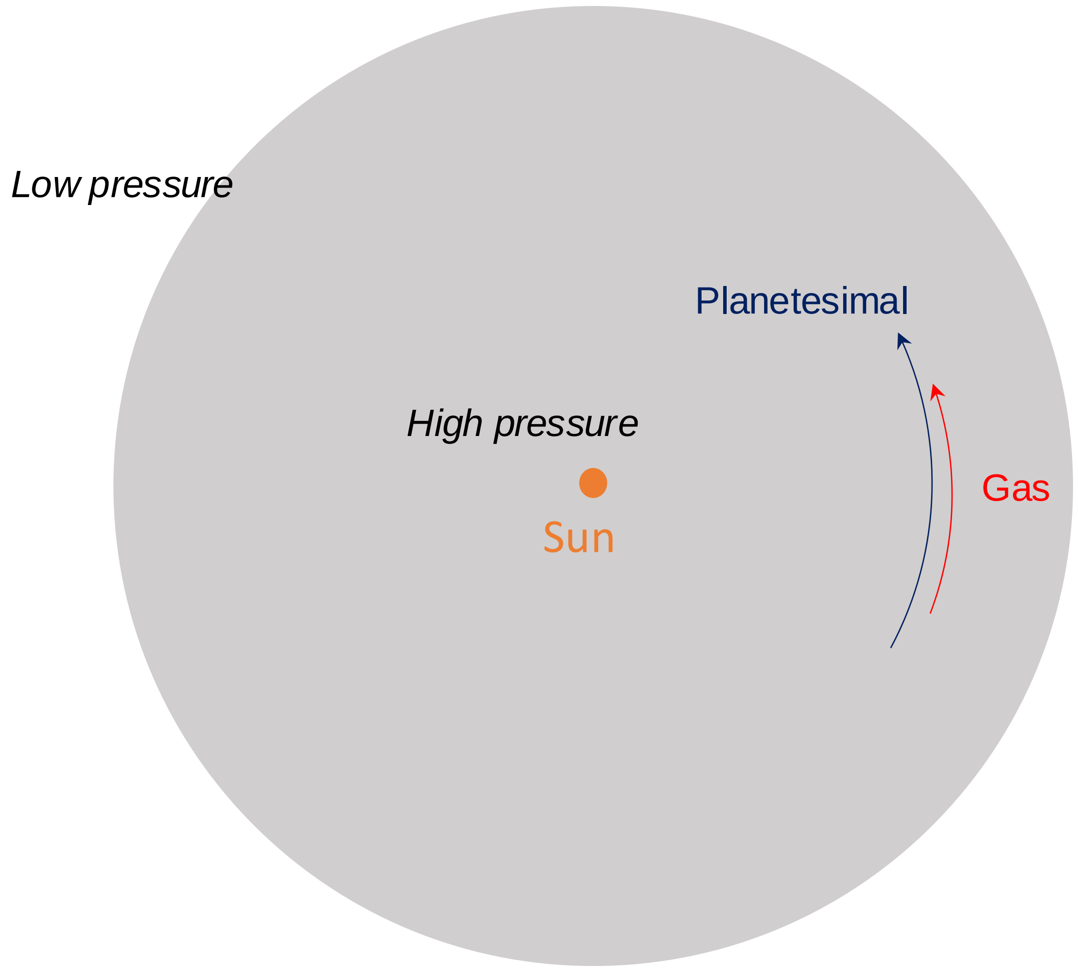

The gas has some pressure support.

The planetesimal has none.

Wind

At initial separation *a* ~ 4000 km:

Binary orbital velocity **~ 0.1 m/s**

Solar orbit velocity at 45AU
$\boldsymbol{v_k}$ **~ 4.5 km/s**

Sub-Keplerian pressure support
$v = v_k\,(1-\eta)$
$\eta \sim 0.01$

Headwind velocity (v_k-v):
ηv ~ 50 m/s

Subkeplerian wind on the binary
= 500 times orbital velocity

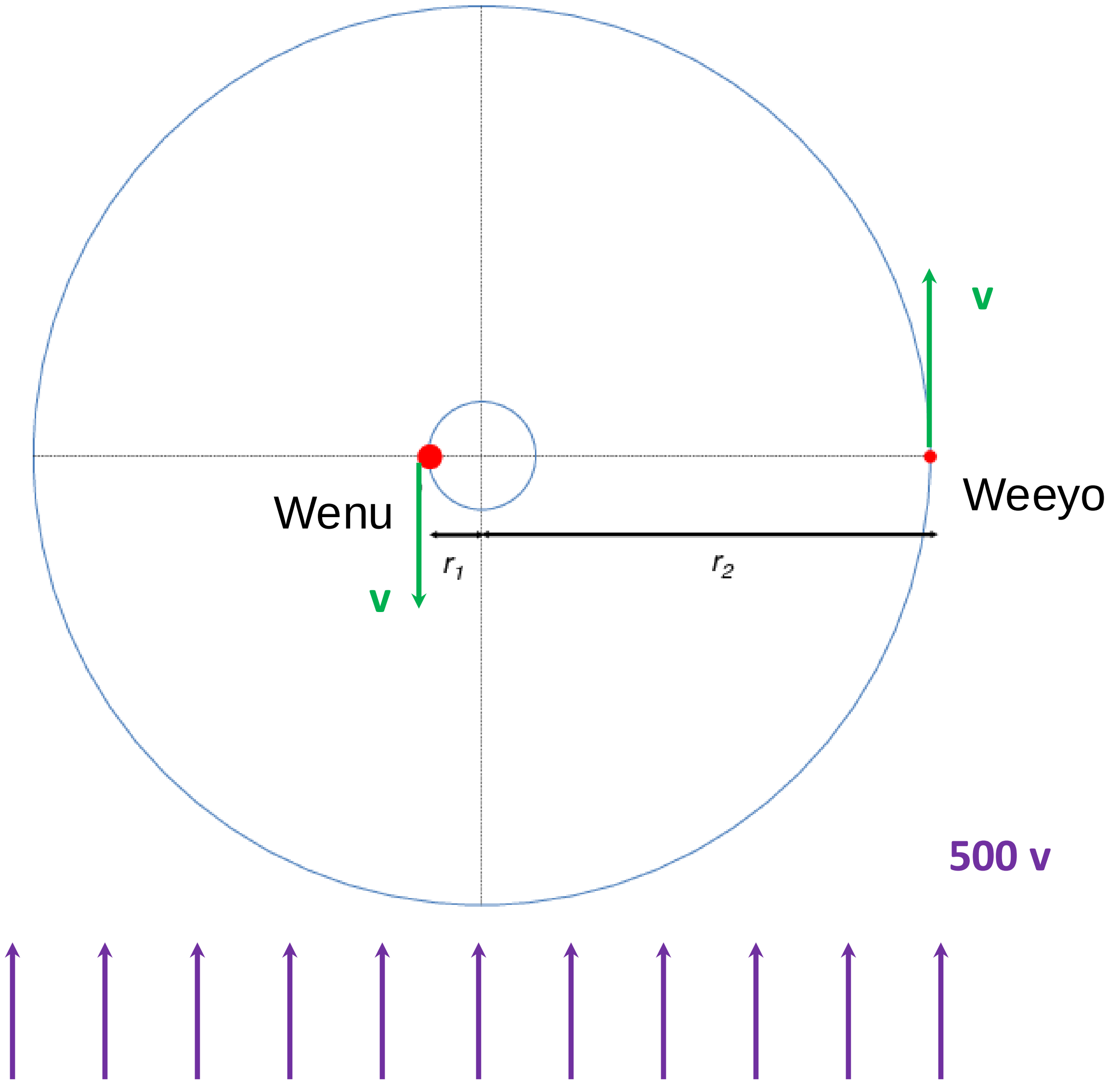

Lyra, Youdin, & Johansen (2021)

Wind solution

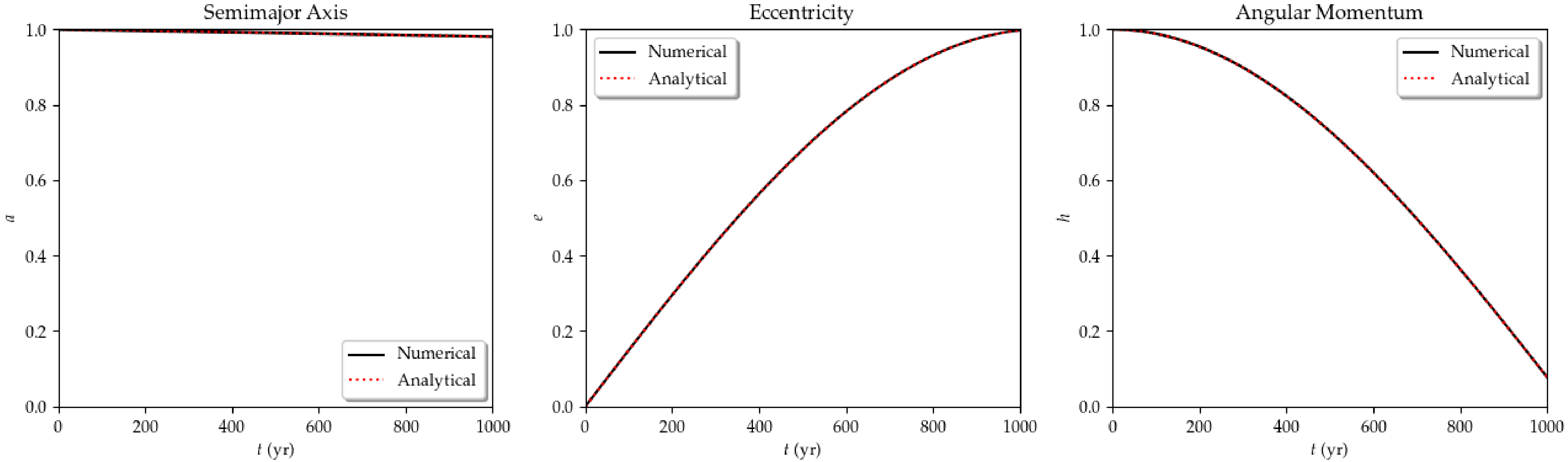

$$\langle a(t)\rangle = a_0 e^{-2t/\tau}$$

$$\langle e(t)\rangle = \cos\left[\cos^{-1} e_0 + \frac{3u}{2}\sqrt{\frac{a_0}{\mu}}\left(1 - e^{-t/\tau}\right)\right]$$

$$\langle h(t)\rangle = e^{-t/\tau}\left\{h_0 - 1 + \cos\left[\frac{3}{2}a_0 u\left(1 - e^{-t/\tau}\right)\right]\right\}$$

W. Lyra

Lyra, Youdin, & Johansen (2021)

Wind solution

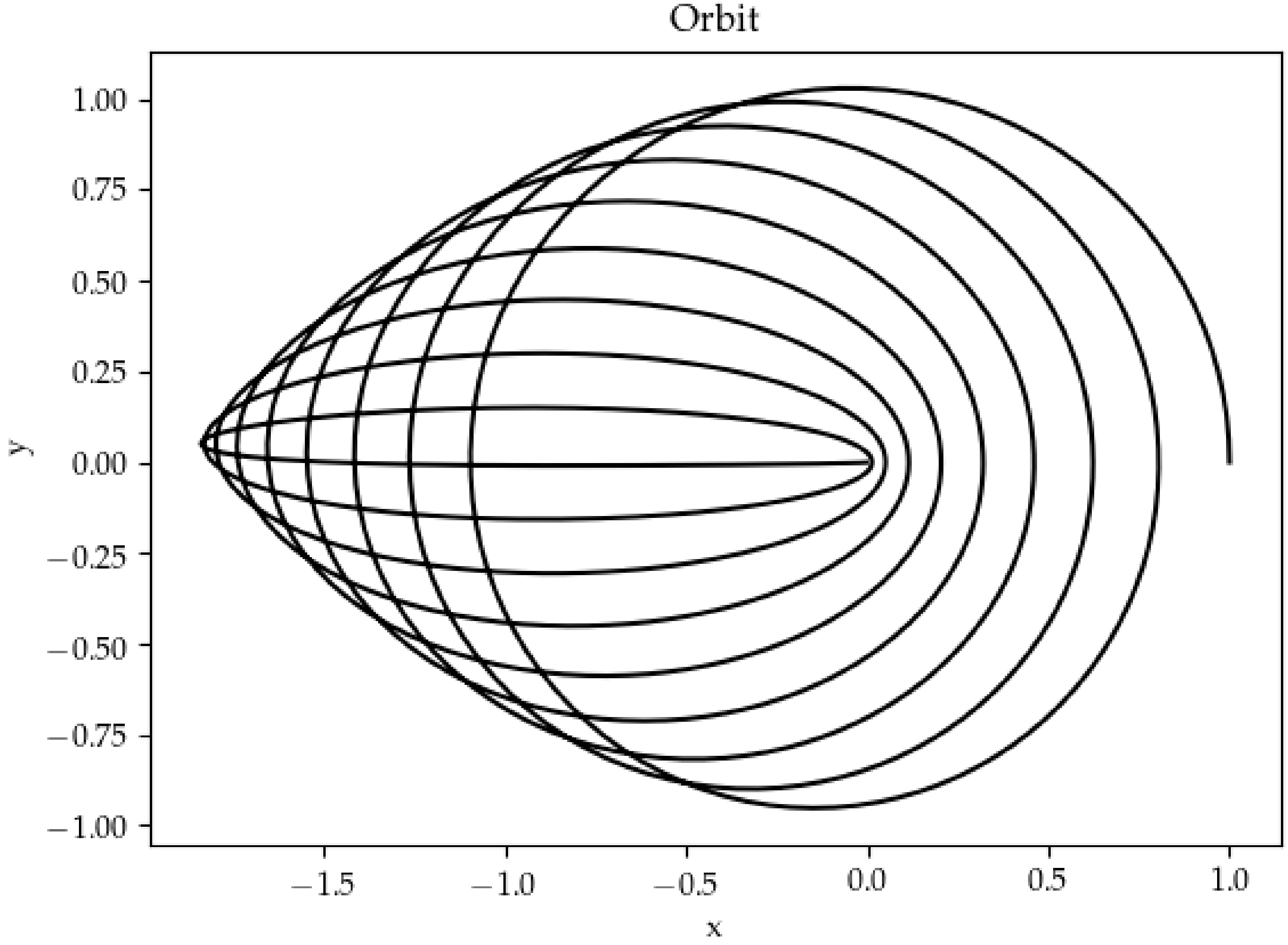

Angular momentum loss at constant energy.

Eccentricity increase at constant semimajor axis

Lyra, Youdin, & Johansen (2021)

Timescales

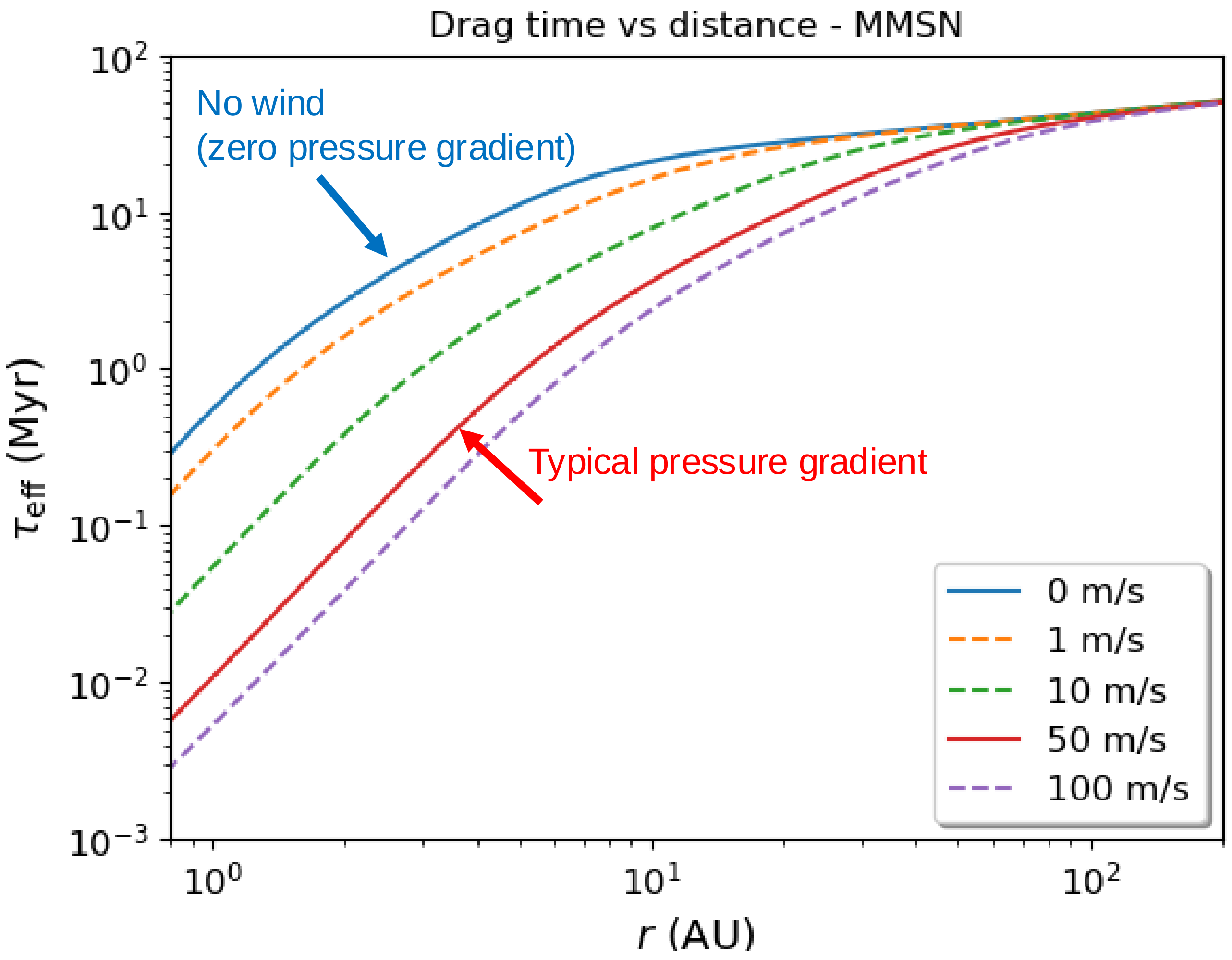

Wind has a strong effect in the distances of the asteroid belt.

Little effect in the Kuiper belt.

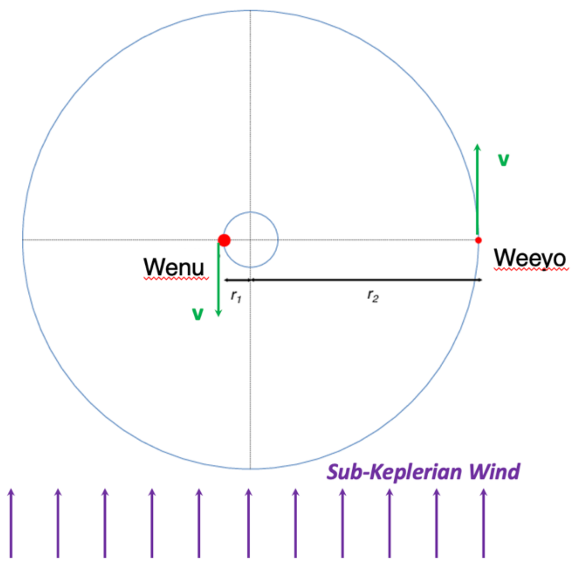

Lyra, Youdin, & Johansen (2021)

Linear vs quadratic drag

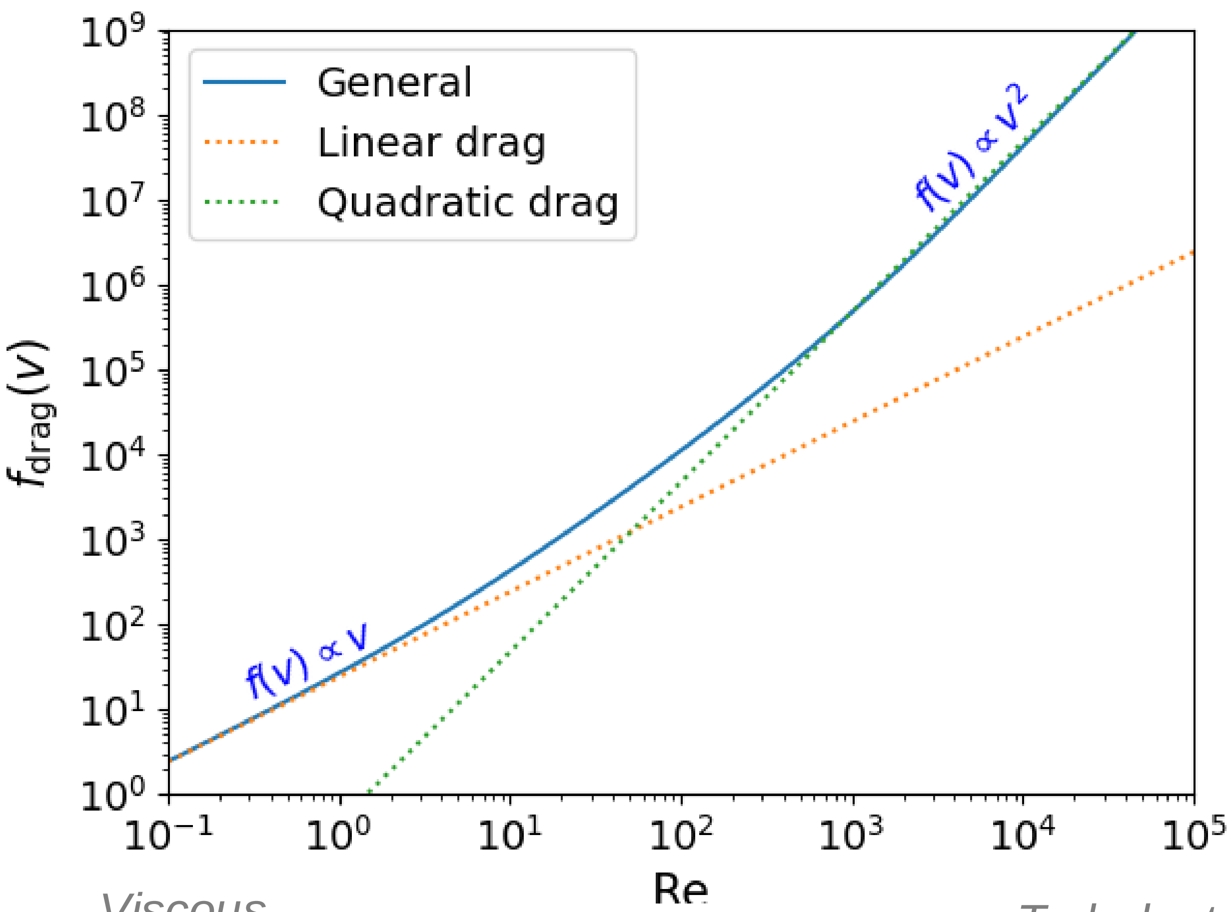

Viscous

Turbulent

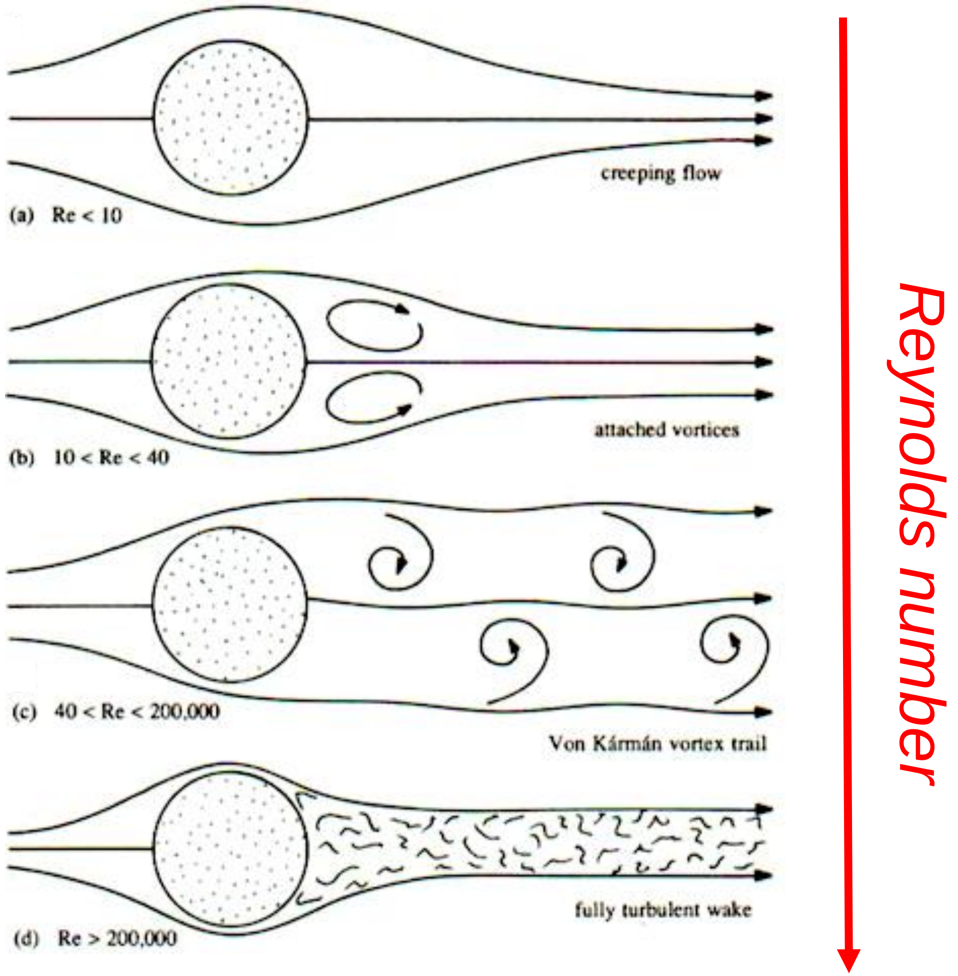

Lyra, Youdin, & Johansen (2021)

The Astrophysical Journal, 733:56 (9pp), 2011 May 20 doi:10.1088/0004-637X/733/1/56

WIND-SHEARING IN GASEOUS PROTOPLANETARY DISKS AND THE EVOLUTION OF BINARY PLANETESIMALS

Hagai B. Perets and Ruth A. Murray-Clay
Harvard-Smithsonian Center for Astrophysics, 60 Garden Street Cambridge, MA 02338, USA
Received 2010 December 13; accepted 2011 March 18; published 2011 May 4

3.2.1. Linear Drag Regime

In the following treatment, we assume that $v_{\rm bin}$ remains constant over a single binary orbital period $P_{\rm bin}$, which is good for $v_{\rm bin}/\dot{v}_{\rm bin} \gg P_{\rm bin}$. Note that this assumption requires not only that $\tau_{\rm merge} \gg P_{\rm bin}/2$ but also that $m_s v_{\rm bin}/F_{D,{\rm disk}} \gg P_{\rm bin}$, where $F_{D,{\rm disk}}$ is the drag force experienced by the small body moving at relative velocity $v_{\rm disk}$ with respect to the gas. We address the complication of non-circular orbits in future work.

In the linear regime, $F_D \propto v_{\rm rel}$, with $v_{\rm rel}$ equal to the relative velocity of the small body with respect to the gas, containing components from the binary orbit and from the overall motion of the binary through the gas disk. Therefore, $F_{D,1} \equiv F_D/v_{\rm rel}$ is constant over the binary orbit. The linear regime is valid for the Epstein and Stokes drag regimes, but the value of $F_{D,1}$ in the two regimes differs (see Section 2.1). We may now express the orbit-averaged drag force as

$$\langle F_D \rangle = \frac{1}{2\pi}\int_0^{2\pi} F_D\, d\theta$$
$$= \frac{F_{D,1}}{2\pi}\int_0^{2\pi} (v_{\rm bin}\sin\theta + v_{\rm disk})\, d\theta = F_{D,1} v_{\rm bin}, \quad (21)$$

wind averages out

where θ is the angle of the binary in its orbit. The term $v_{\rm bin}\sin\theta$ is the bulk velocity component of the small planetesimal parallel to the direction of motion in the binary frame of reference, so that $v_{\rm rel} = v_{\rm bin}\sin\theta + v_{\rm disk}$. Over a full orbit the contribution from $v_{\rm disk}$ averages out and

$$\tau_{\rm merge} = \frac{t_{\rm stop}}{2}, \quad (22)$$

with $t_{\rm stop}$ equal to the stopping time of a single small planetesimal in the gaseous protoplanetary disk:

$$t_{\rm stop} = \frac{m_s}{F_{D,1}} = \begin{cases} \left(\frac{\rho_p}{\rho_g}\right)\frac{r_s}{\bar{v}_{\rm th}} & \text{Epstein} \\ \frac{4}{9}\left(\frac{\rho_p}{\rho_g}\right)\frac{r_s^2}{\lambda \bar{v}_{\rm th}} & \text{Stokes.} \end{cases}$$

Recall that in the linear regime, the stopping time is independent of the relative velocity between the planetesimal and the gas. Note that single planetesimals with stopping times longer than an orbital time inspiral into the star on a timescale of $\sim t_{\rm stop}/\eta$. The same processes are at work in both cases—infall into the star is slower than binary coalescence because the gas and planetesimals orbit the star together, reducing their relative velocities.

The timescale for coalescence is independent of $d_{\rm bin}$, and the total merger time for a binary is

$$T_{\rm merge} = \tau_{\rm merge} \ln\left(\frac{d_0}{r_b}\right), \quad (23)$$

where $d_{\rm bin} = d_0$ initially, and r_b is the final binary separation before coalescence.

3.2.2. Quadratic (Ram Pressure) Regime

We now consider the quadratic regime, for which $F_D \propto v_{\rm rel}^2$, appropriate for ram pressure drag. Following the same procedure as above, but using $F_{D,2} \equiv F_D/v_{\rm rel}^2$ with $F_{D,2}$ a constant, we get

$$\langle F_D \rangle = \frac{F_{D,2}}{2\pi}\int_0^{2\pi} (v_{\rm bin}\sin\theta + v_{\rm disk})^2 d\theta$$
$$= F_{D,2} v_{\rm bin}^2 \left[1 + \frac{1}{2}\left(\frac{v_{\rm disk}}{v_{\rm bin}}\right)^2\right]. \quad (24)$$

wind doesn't average out

In other words, the ram pressure drag force requires an effective relative velocity correction of $[1+0.5(v_{\rm disk}/v_{\rm bin})^2]$—in this case the contribution from the bulk velocity drag did not average out.

Now,

$$\tau_{\rm merge} = \frac{t_{\rm stop}(v_{\rm bin})/2}{1+0.5(v_{\rm disk}/v_{\rm bin})^2}, \quad (25)$$

where $t_{\rm stop}(v_{\rm bin})$ is the stopping time for $v_{\rm rel} = v_{\rm bin}$. In the quadratic regime, $t_{\rm stop}$ is not independent of $v_{\rm rel}$, so to make dependences clearer, we rewrite this expression as

$$\tau_{\rm merge} = \frac{m_s/(2F_{D,2})}{v_{\rm bin}[1+0.5(v_{\rm disk}/v_{\rm bin})^2]} \approx \begin{cases} \frac{m_s}{2F_{D,2}v_{\rm bin}}, & v_{\rm bin} \gg v_{\rm disk} \\ \frac{m_s v_{\rm bin}}{F_{D,2}v_{\rm disk}^2}, & v_{\rm bin} \ll v_{\rm disk} \end{cases}. \quad (26)$$

Plugging in $F_{D,2}$ for ram pressure drag and $v_{\rm bin} = (Gm_b/d_{\rm bin})^{1/2}$, this corresponds to

$$\tau_{\rm merge} \approx \frac{2}{0.66}\left(\frac{\rho_p}{\rho_g}\right) r_s \times \begin{cases} d_{\rm bin}^{1/2}/\sqrt{Gm_b}, & v_{\rm bin} \gg v_{\rm disk} \\ 2\sqrt{Gm_b}/(d_{\rm bin}^{1/2} v_{\rm disk}^2), & v_{\rm bin} \ll v_{\rm disk} \end{cases}. \quad (27)$$

W. Lyra

Perets & Murray-Clay (2011)

Linear vs quadratic drag

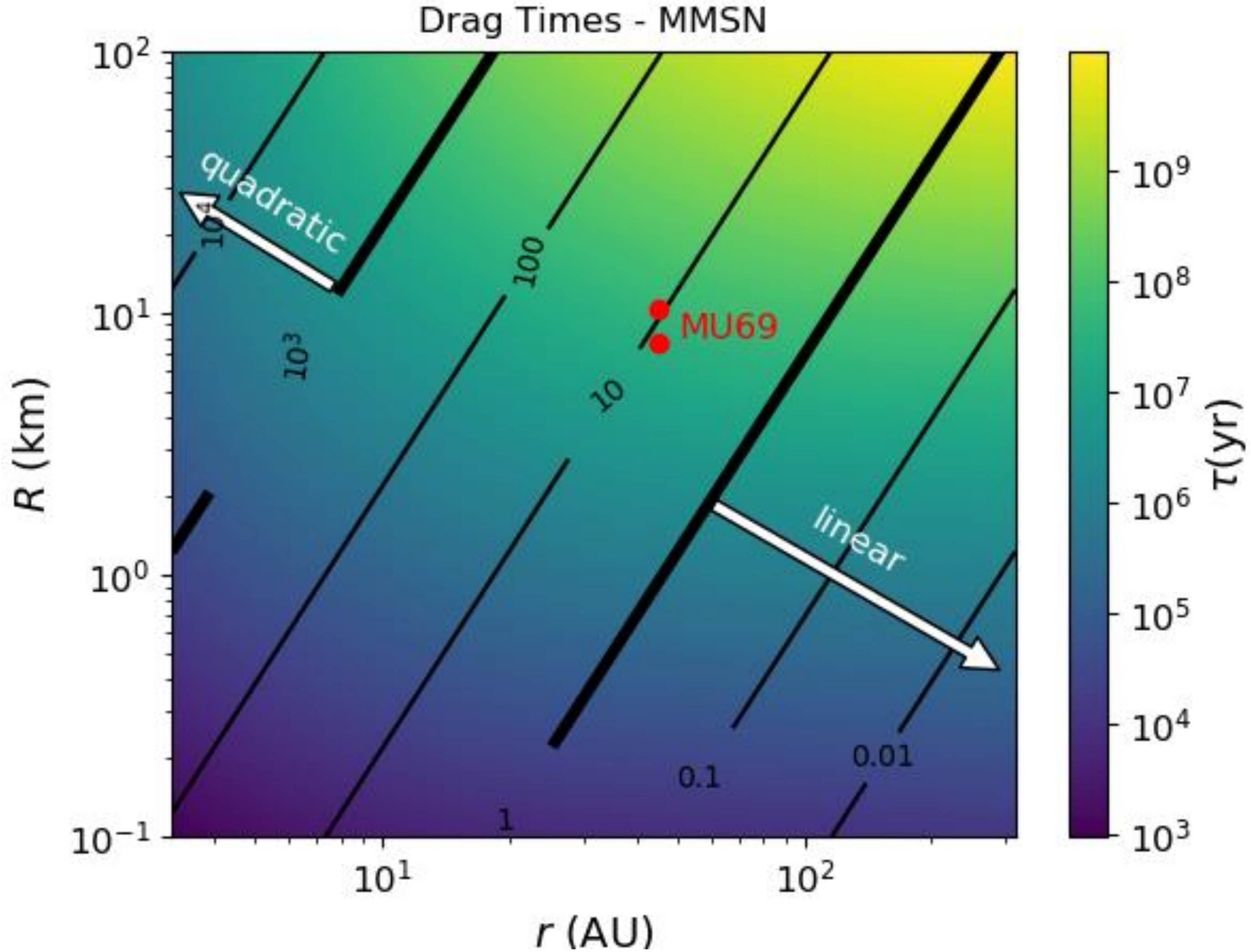

Lyra, Youdin, & Johansen (2021)

McKinnon et al. (2020) considers only quadratic drag

Science

Current Issue First release papers Archive About Submit man

HOME > SCIENCE > VOL. 367, NO. 6481 > THE SOLAR NEBULA ORIGIN OF (486958) ARROKOTH, A PRIMORDIAL CONTACT BINARY IN THE KUIPER BELT

RESEARCH ARTICLE

The solar nebula origin of (486958) Arrokoth, a primordial contact binary in the Kuiper Belt

W. B. MCKINNON, D. C. RICHARDSON, J. C. MAROHNIC, J. T. KEANE, W. M. GRUNDY, D. P. HAMILTON, D. NESVORNÝ, O. M. UMURHAN, T. R. LAUER, [...], AND THE NEW HORIZONS SCIENCE TEAM +19 authors Authors Info & Affiliations

SCIENCE • 13 Feb 2020 • Vol 367, Issue 6481 • DOI: 10.1126/science.aay6620

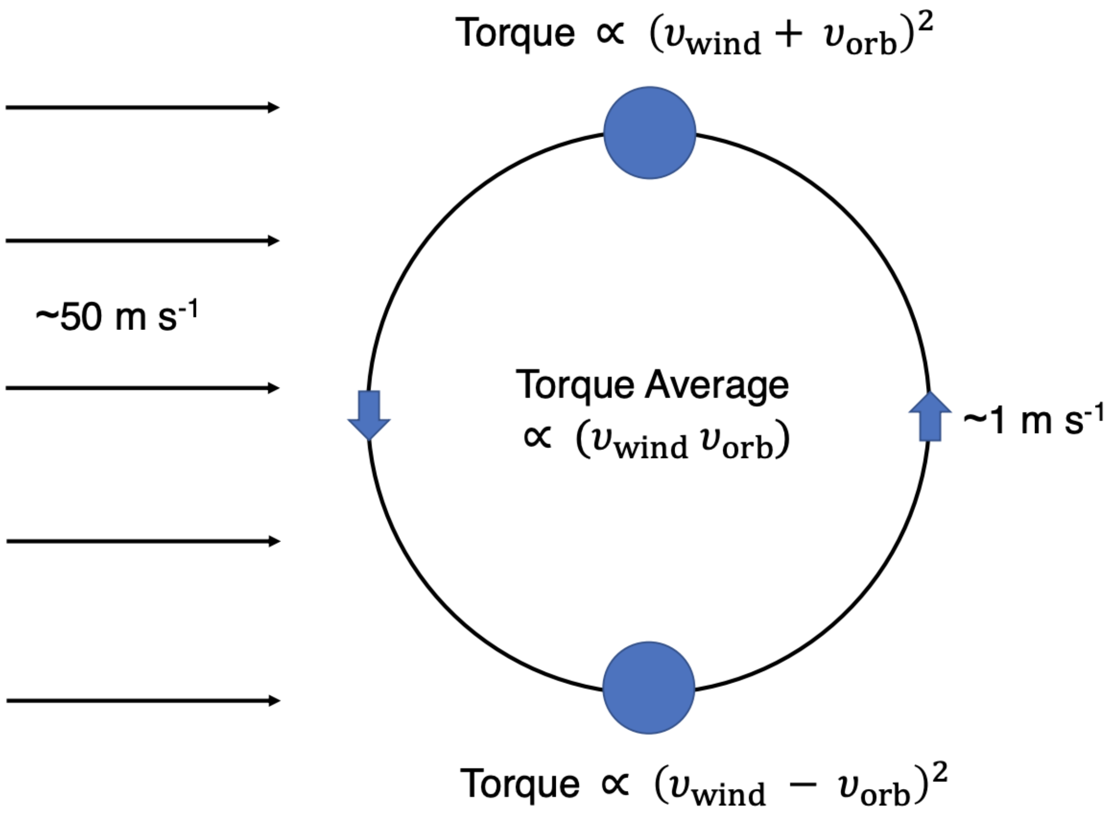

Fig. 7. Illustration of the protosolar nebula headwind interacting with a co-orbiting equal mass binary. The averaged torque is proportional to the product of the lobe orbital velocity and the differential velocity between the nebular gas and the binary's center-of-mass about the Sun.

McKinnon et al. (2020)

At the linear range

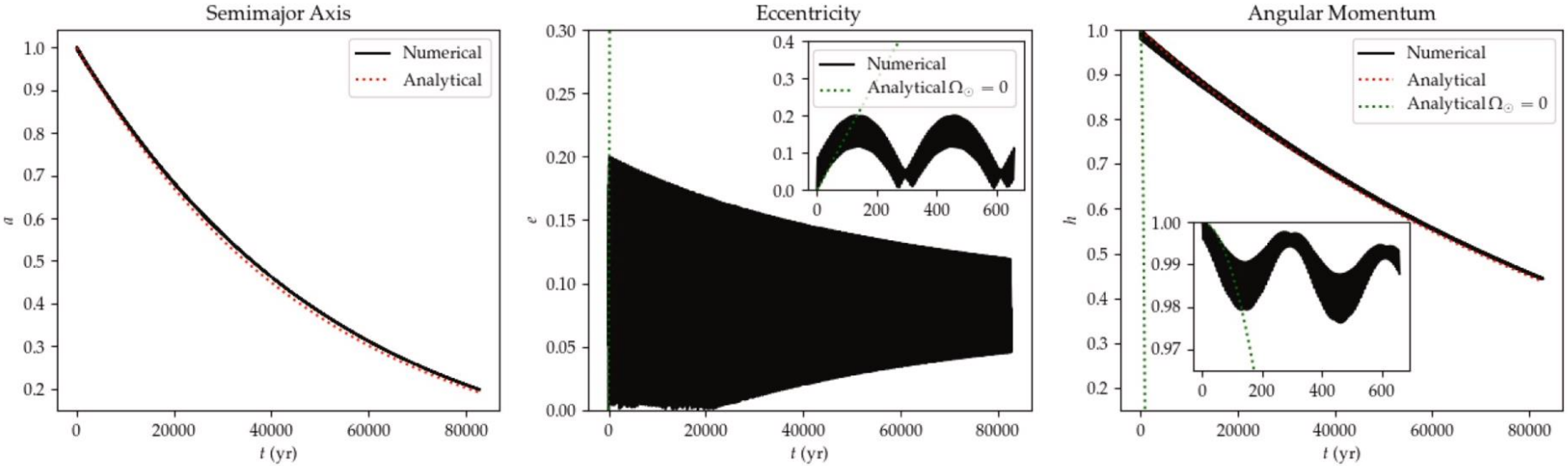

The average reverts to the no-wind solution:

$$h = h_0 e^{-t/\tau_{\rm eff}},$$

$$a = a_0\, e^{-2t/\tau_{\rm eff}}$$

e = const

Lyra, Youdin, & Johansen (2021)

More massive nebula?

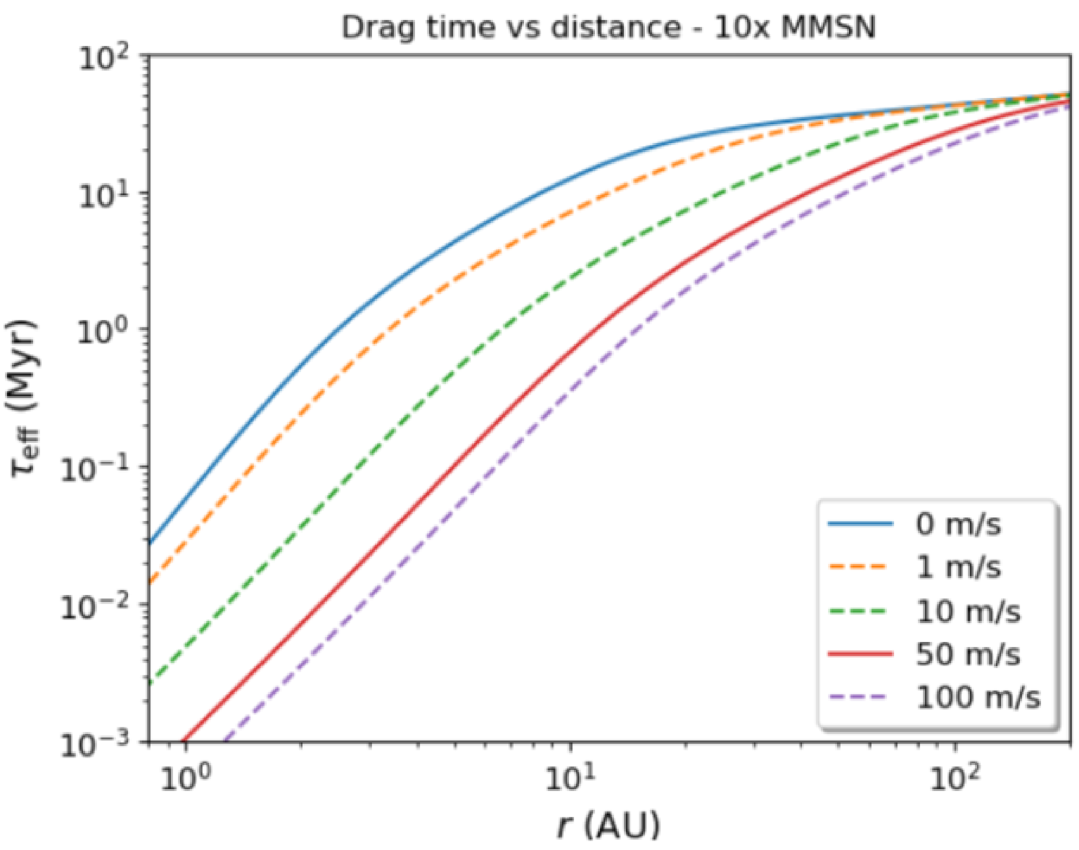

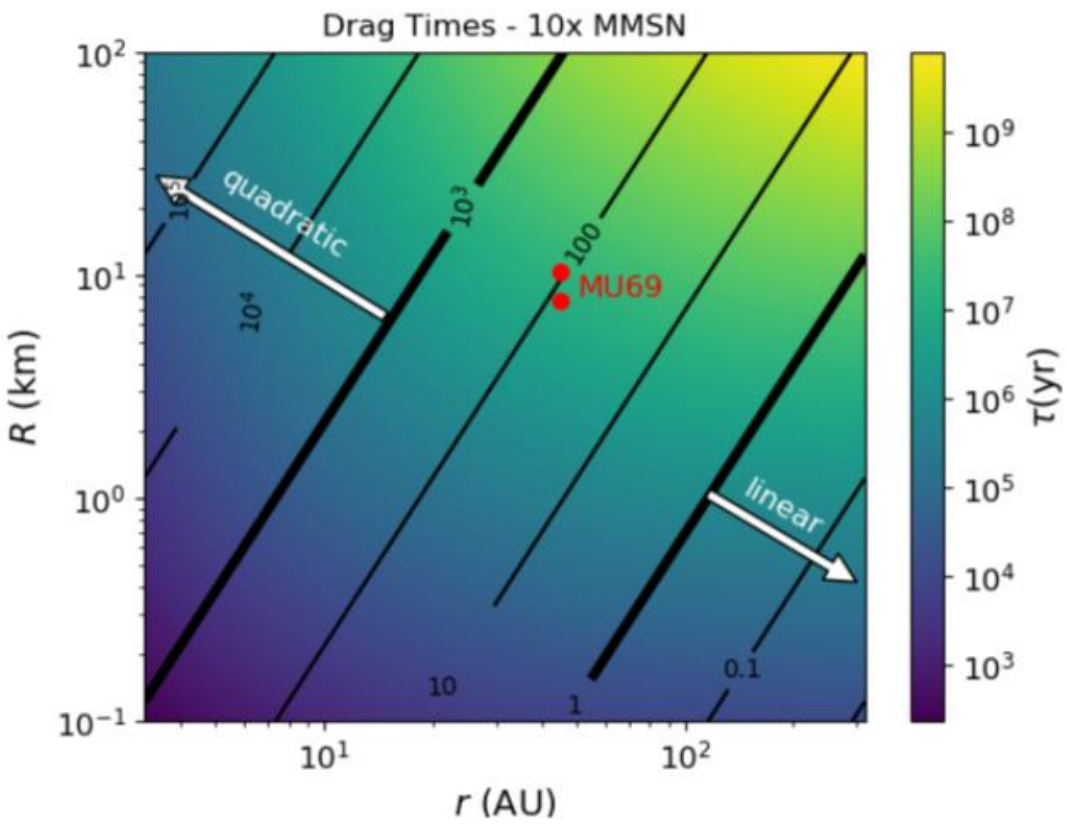

Close but no cigar.

Lyra, Youdin, & Johansen (2021)

Inclination 99.3^o

Effect of Inclination

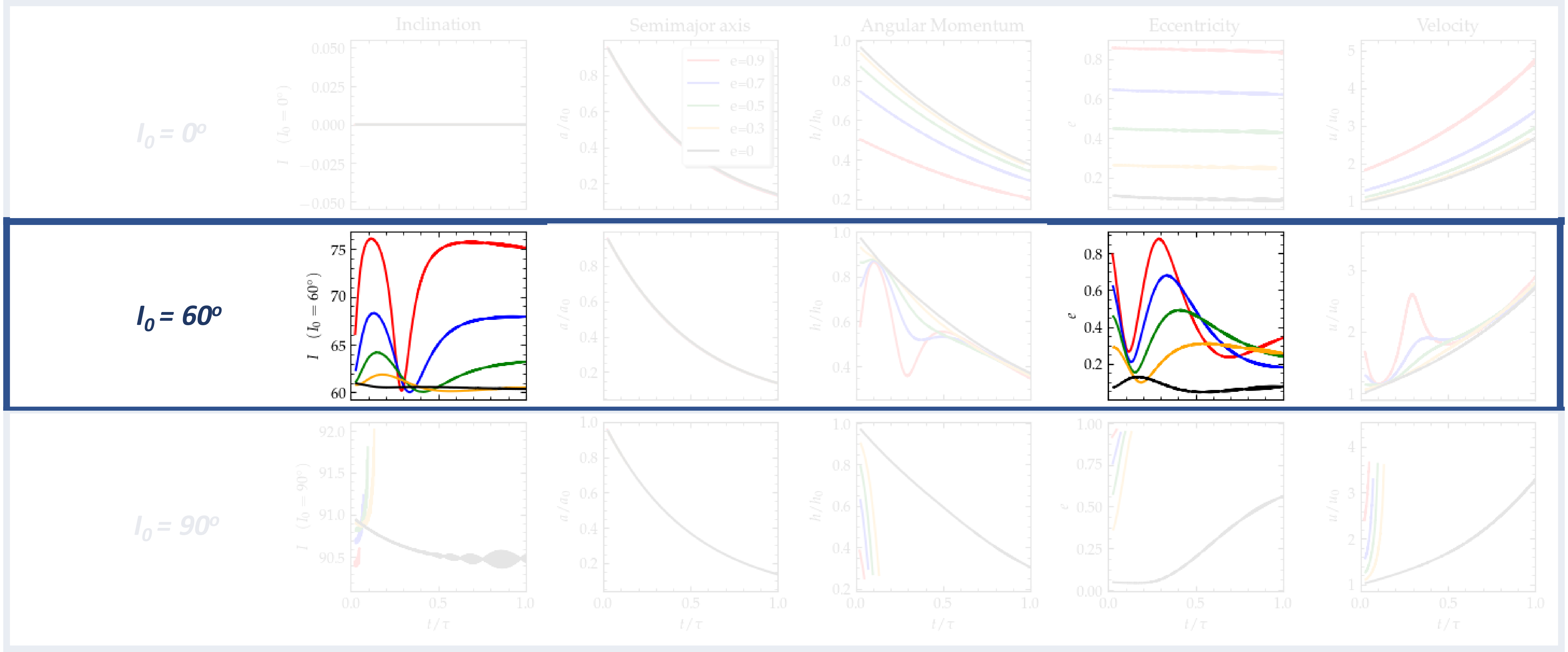

Lyra, Youdin, & Johansen (2021)

Kozai-Lidov Oscillations

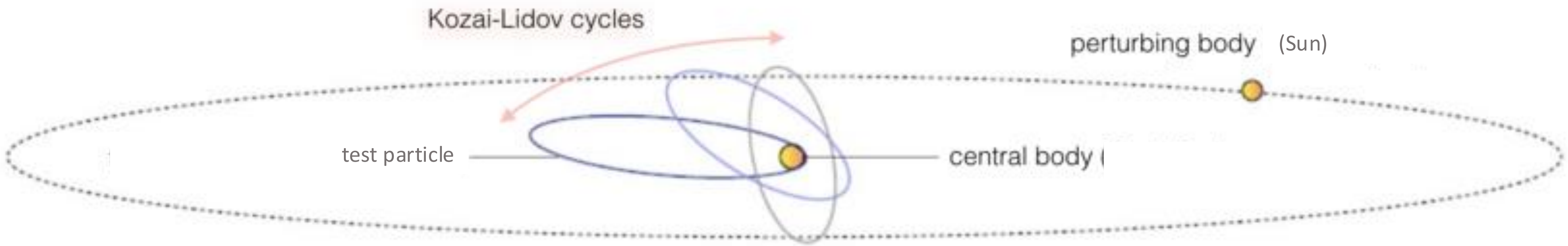

Effect of Inclination

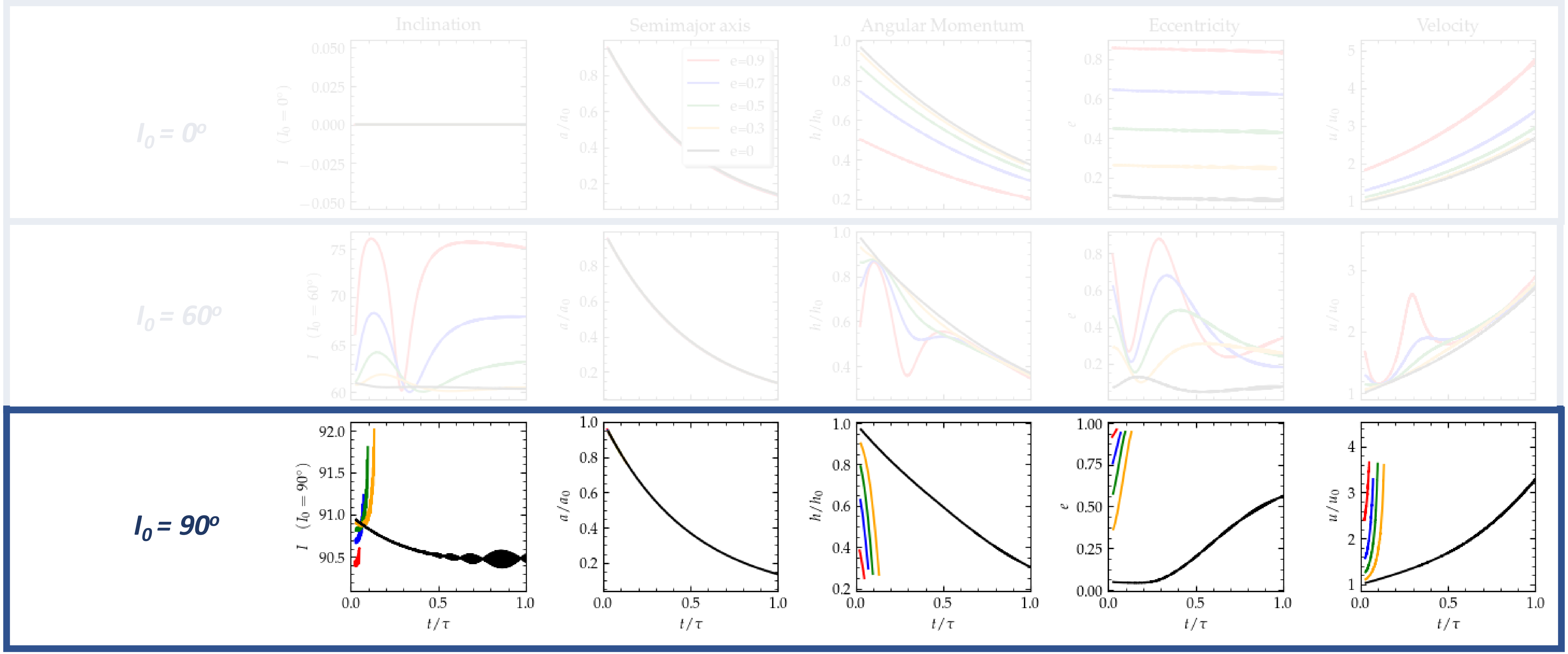

W. Lyra

Lyra, Youdin, & Johansen (2021)

$I_0 = 90^o$ inclination

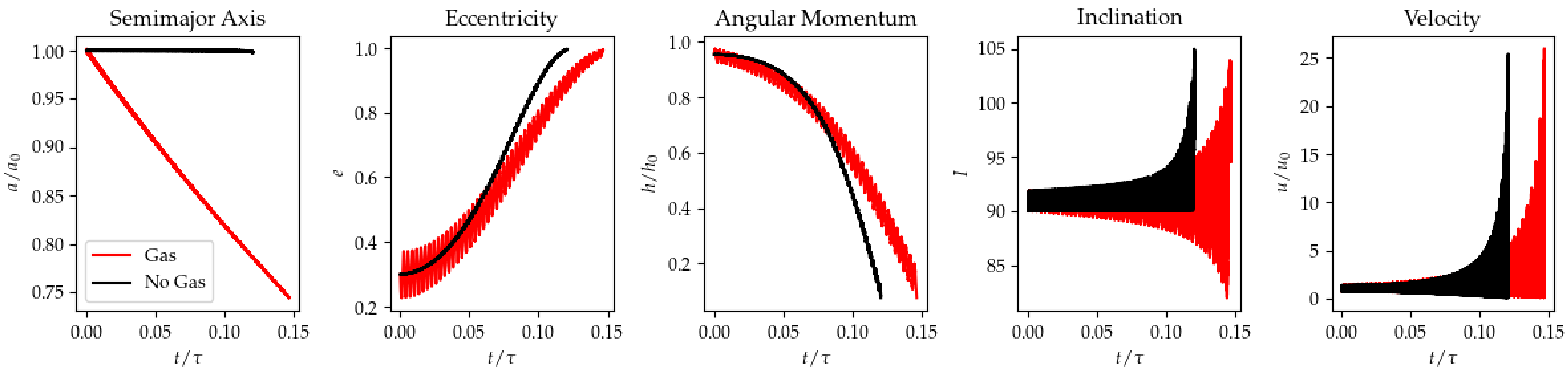

Lyra, Youdin, & Johansen (2021)

Kozai-Lidov Oscillations

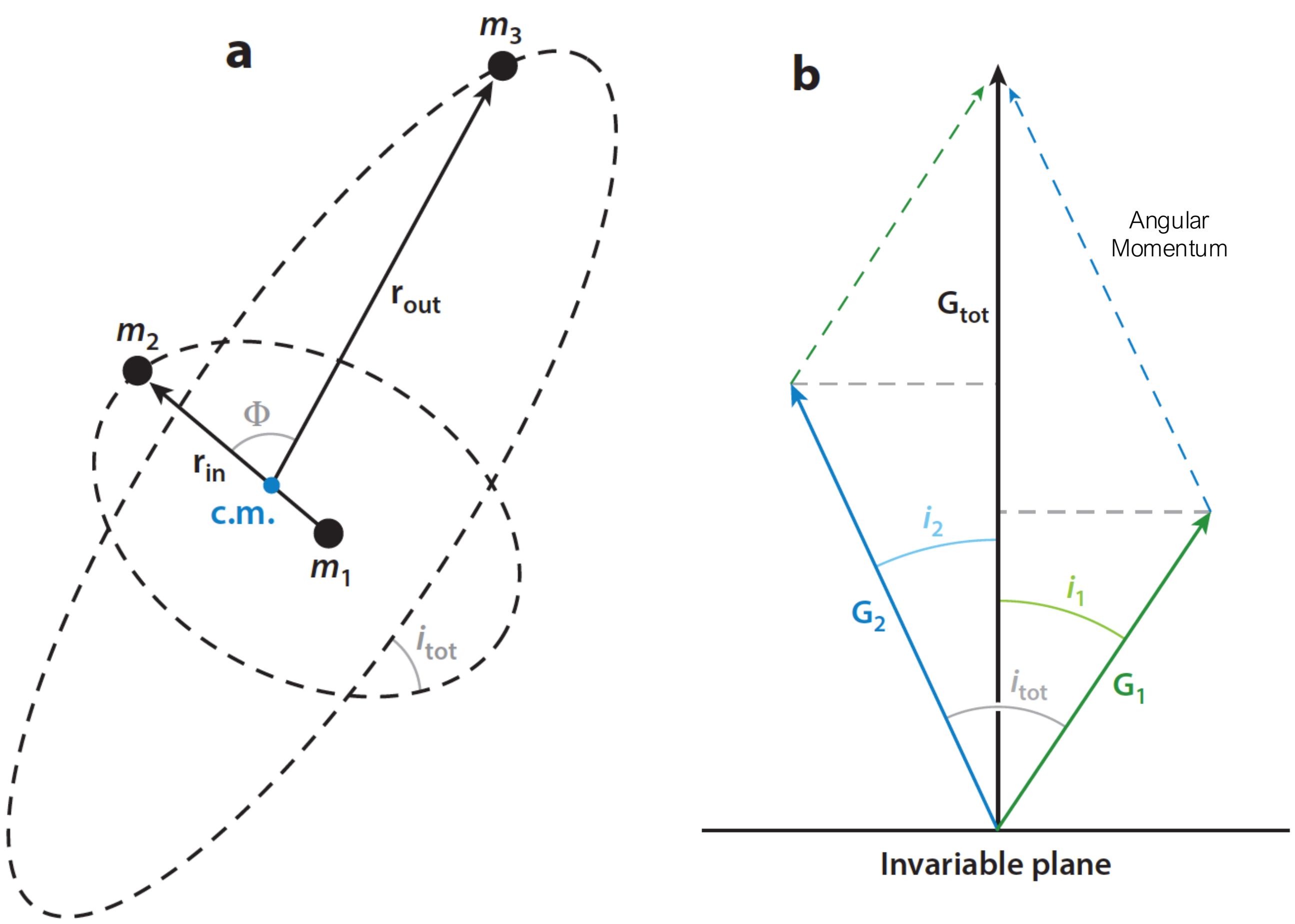

Conserved quantity is not angular momentum, but vertical angular momentum

Conserved quantities:

Energy

$E = -1/(2a)$

Vertical angular momentum

$j_z = (1-e^2)^{1/2} \cos I$

$F = e^2 \left({}^2/_5 - \sin^2 I \sin^2 \omega \right)$

Naoz 2016

Kozai-Lidov Oscillations

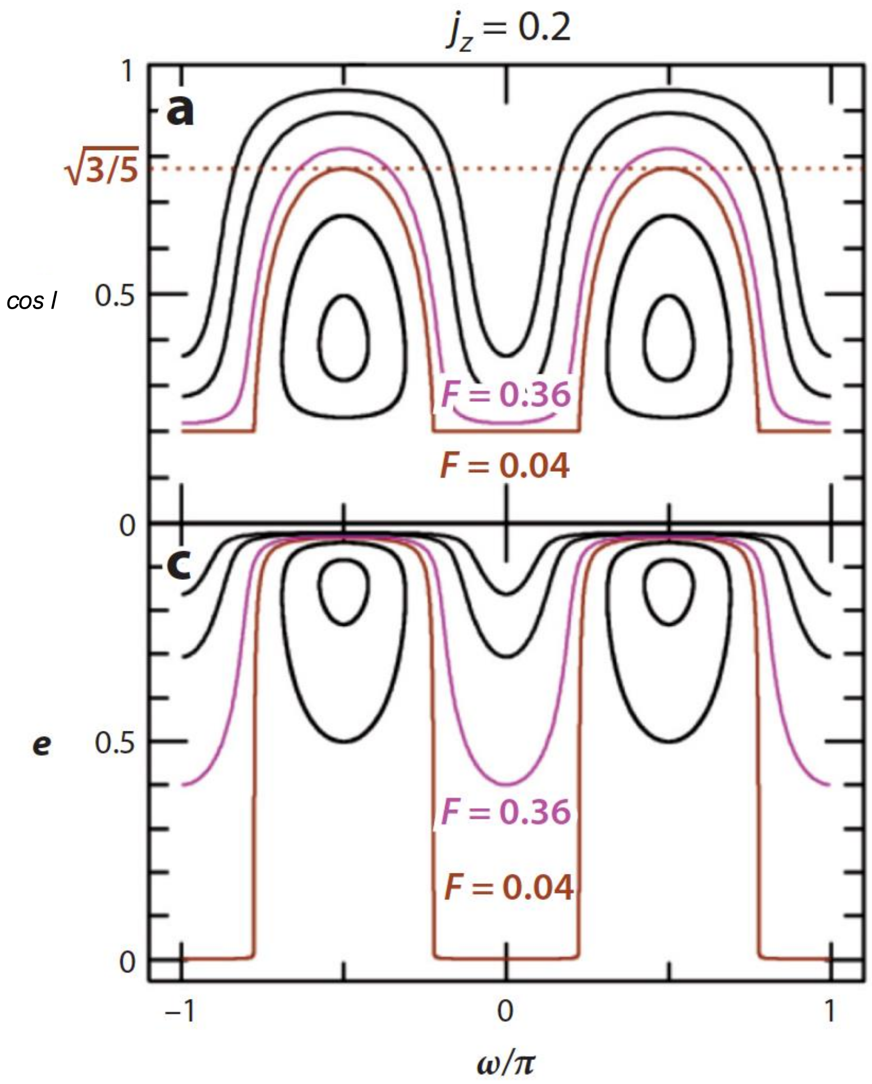

Cycles of inclination and eccentricity

$j_z = (1-e^2)^{1/2} \cos I$

$F = e^2\,(\,^2/_5 - \sin^2 I \sin^2\omega)$

Naoz 2016

Kozai + Tidal Friction + Permanent Quadrupole + Drag

$$
\begin{aligned}
\frac{de}{dt} &= -e\left[V_1 + V_2 + V_d + 5\left(1-e^2\right) S_{eq}\right], \\
\frac{dh}{dt} &= -h\left(W_1 + W_2 + W_d - 5e^2 S_{eq}\right), \\
\frac{d\hat{e}}{dt} &= \left[Z_1 + Z_2 + \left(1-e^2\right)\left(4S_{ee} - S_{qq}\right)\right]\hat{q} \\
&\quad - \left[Y_1 + Y_2 + \left(1-e^2\right) S_{qh}\right]\hat{h}, \\
\frac{d\hat{h}}{dt} &= \left[Y_1 + Y_2 + \left(1-e^2\right) S_{qh}\right]\hat{e} \\
&\quad - \left[X_1 + X_2 + \left(4e^2+1\right) S_{eh}\right]\hat{q}, \\
\frac{d\Omega_1}{dt} &= \frac{\mu_r h}{I_1}\left(-Y_1\hat{e} + X_1\hat{q} + W_1\hat{h}\right), \\
\frac{d\Omega_2}{dt} &= \frac{\mu_r h}{I_2}\left(-Y_2\hat{e} + X_2\hat{q} + W_2\hat{h}\right).
\end{aligned}
$$

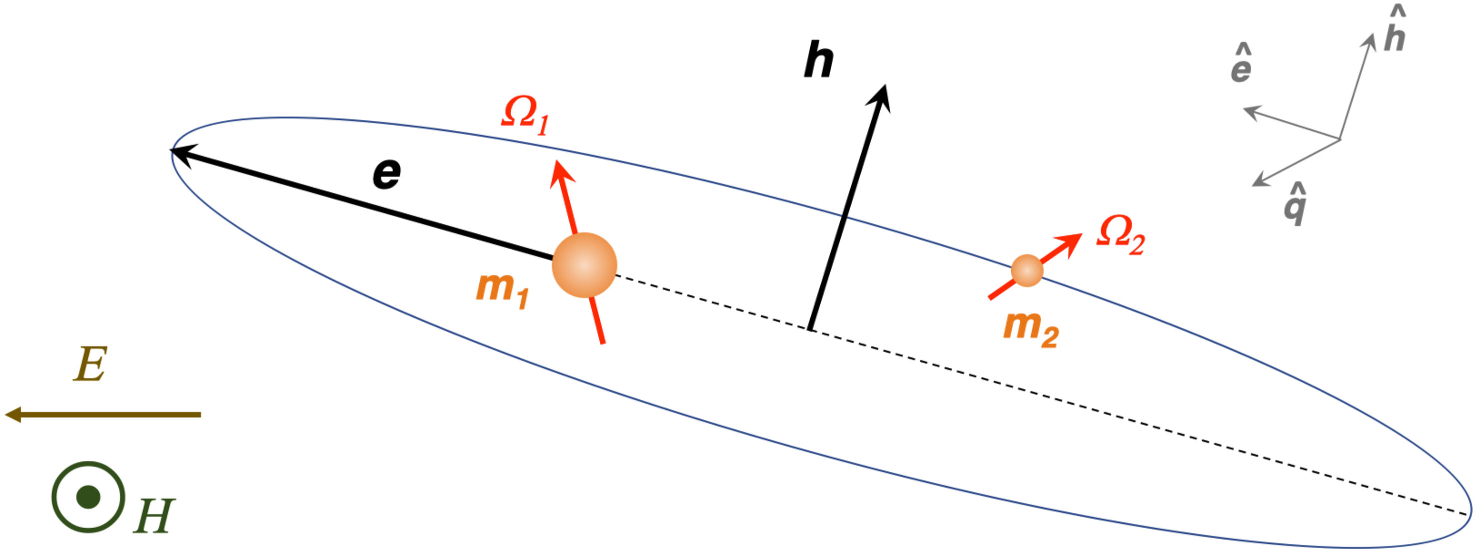

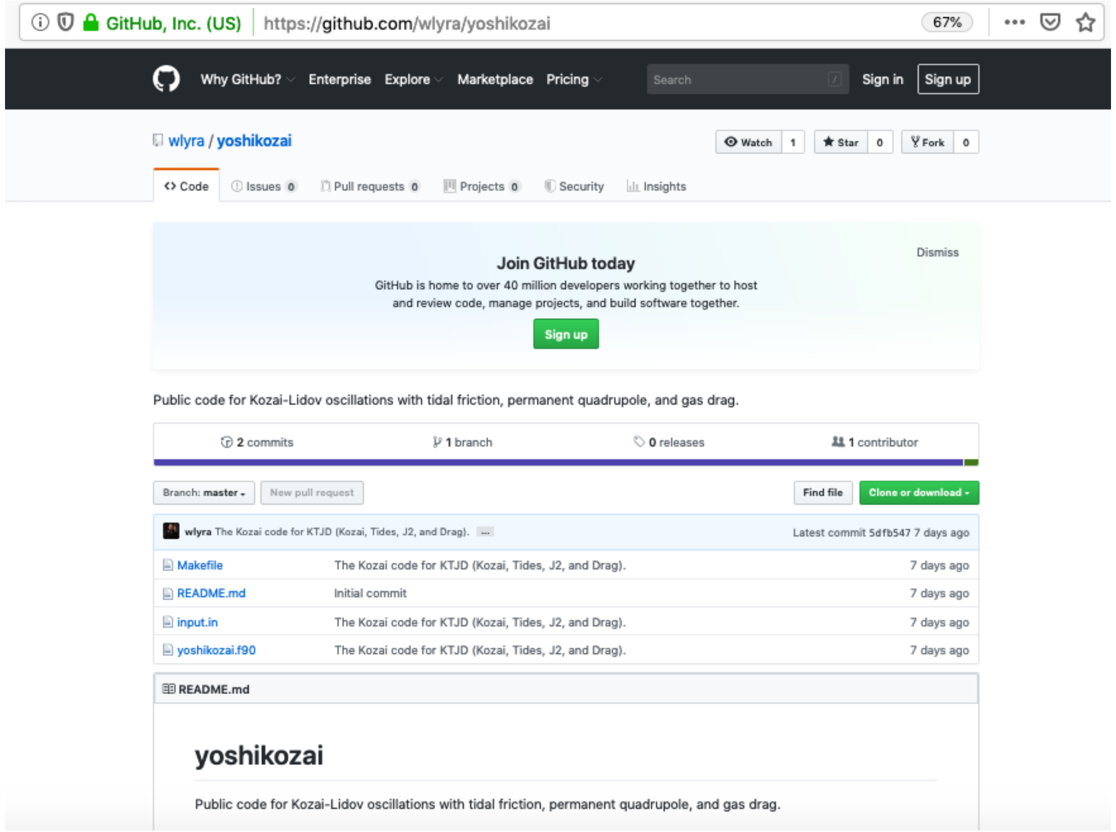

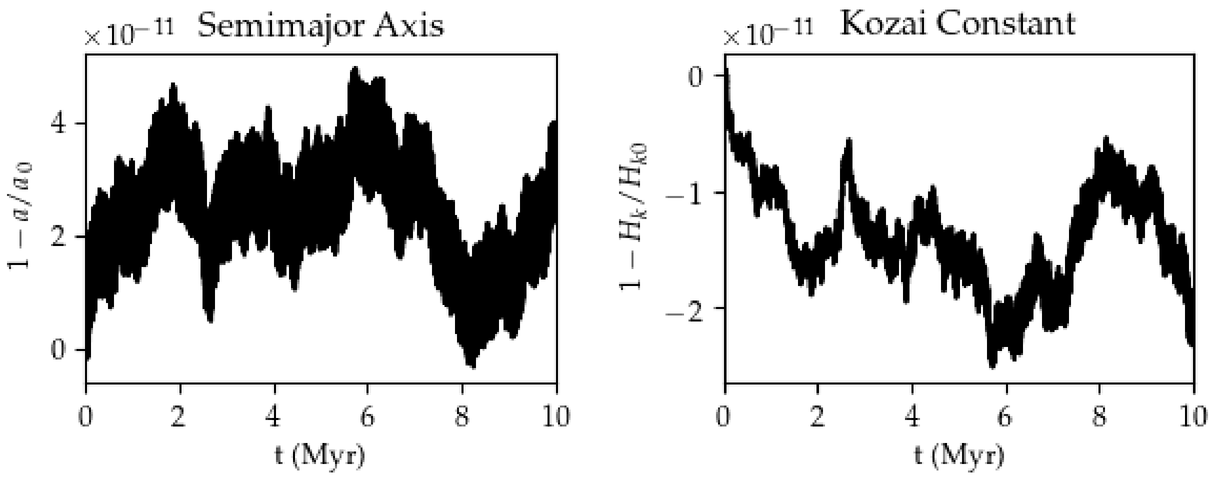

Lyra, Youdin, & Johansen (2021)

Critical Inclination

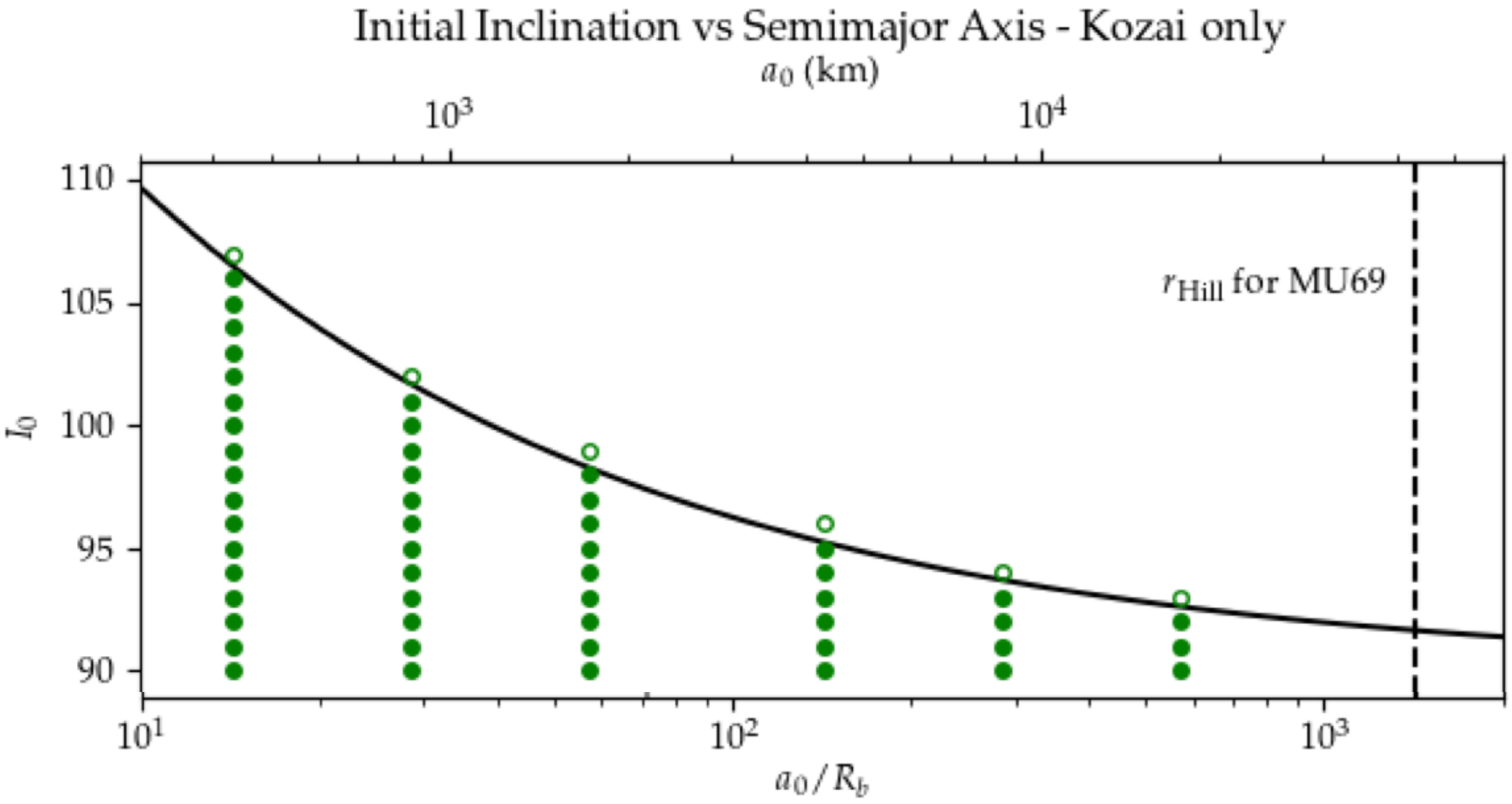

- ● Contact
- ○ No contact

Lyra, Youdin, & Johansen (2021)

Kozai + Tidal Friction + Drag

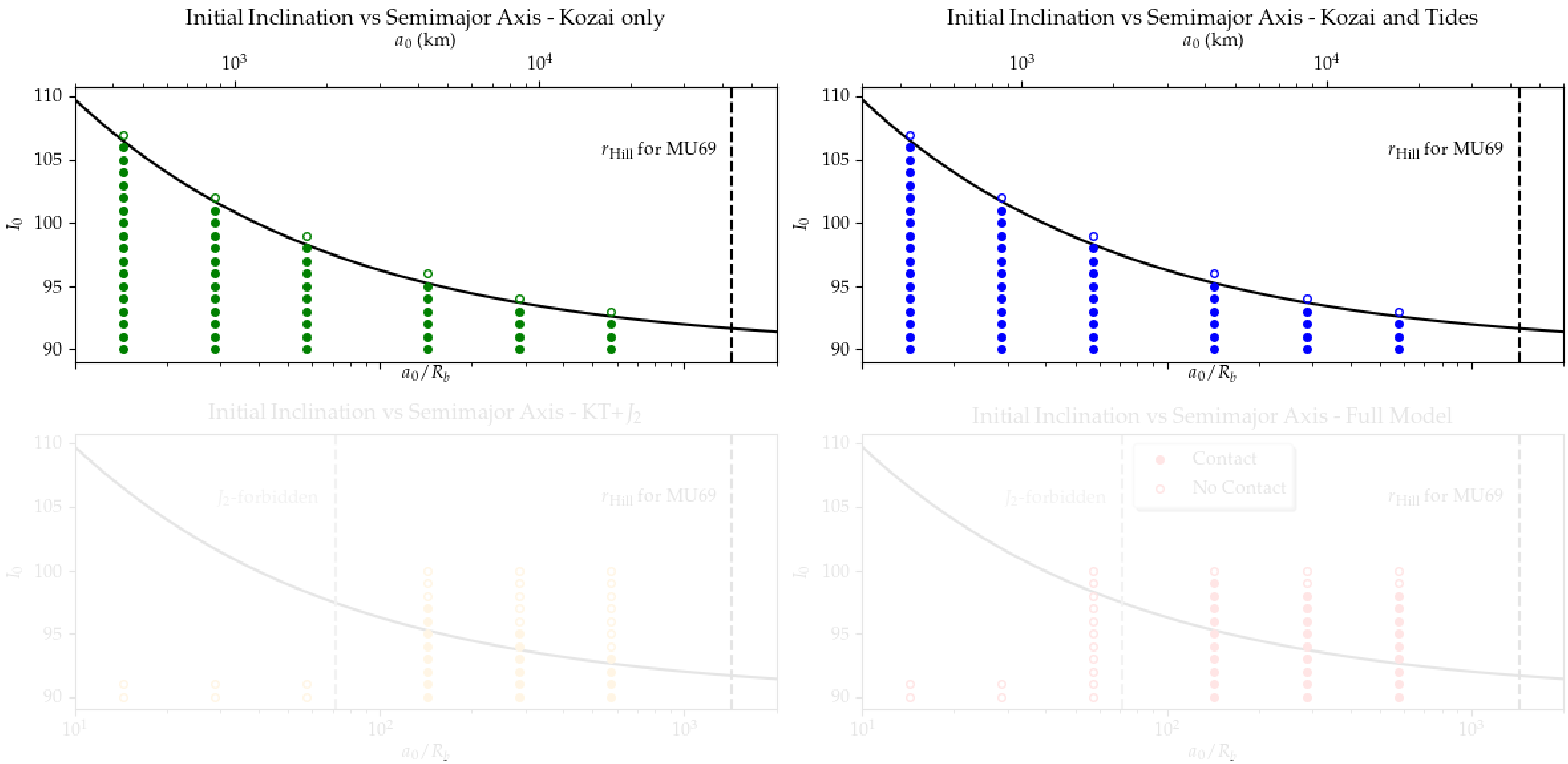

W. Lyra

Lyra, Youdin, & Johansen (2021)

Kozai + Tidal Friction + Drag

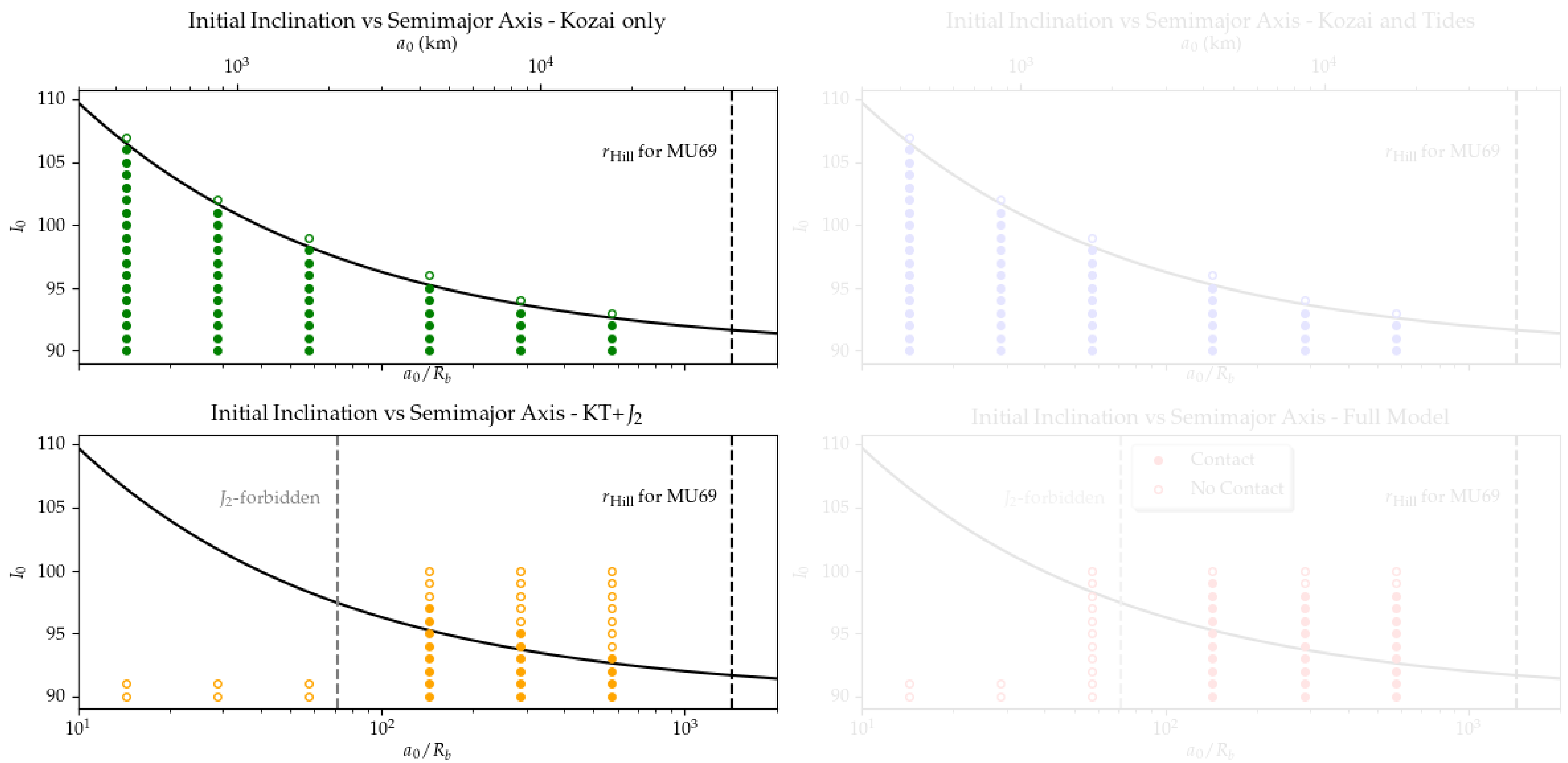

W. Lyra

Lyra, Youdin, & Johansen (2021)

Kozai + Tidal Friction + Drag

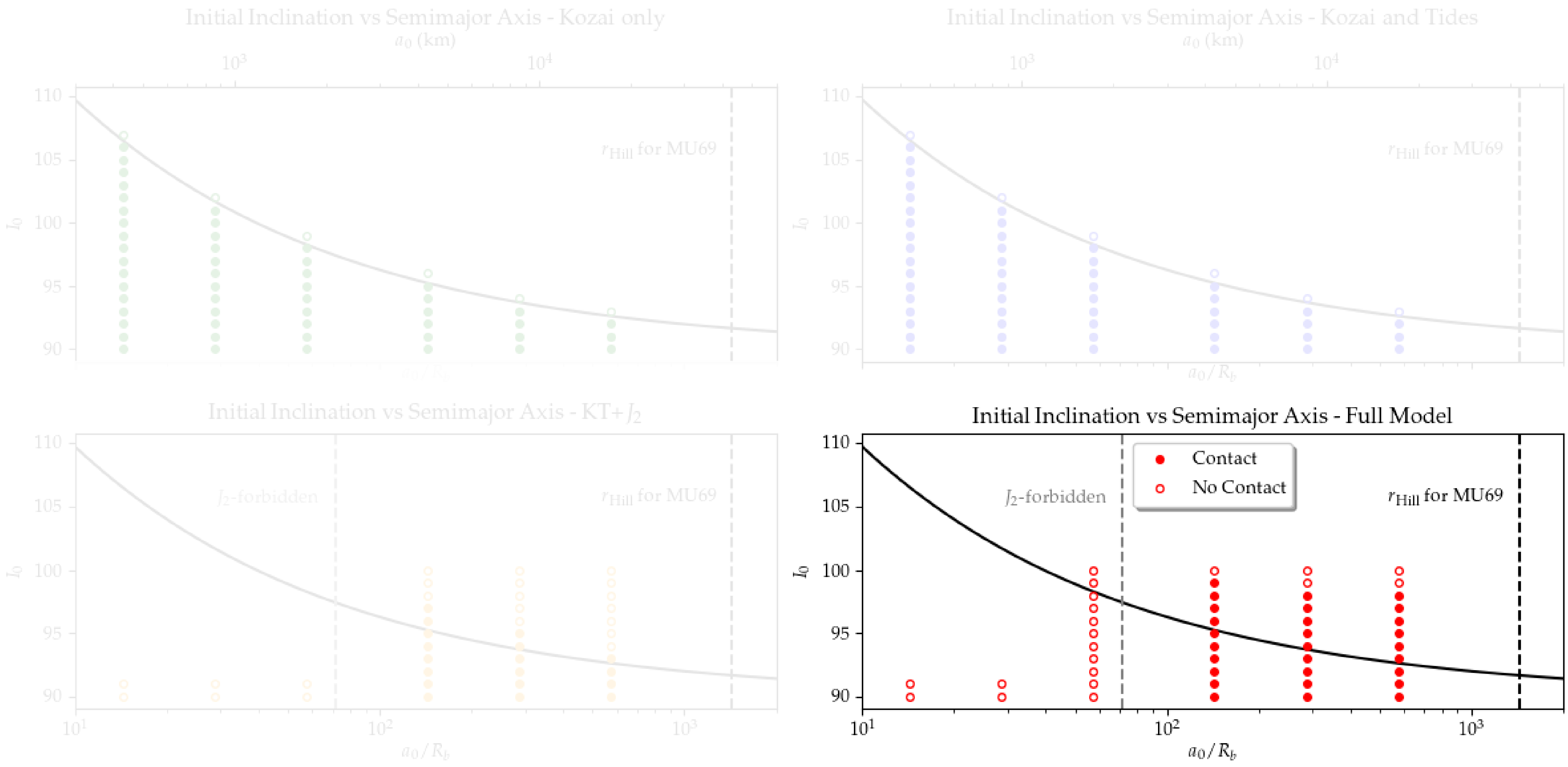

Lyra, Youdin, & Johansen (2021)

Effect of Drag

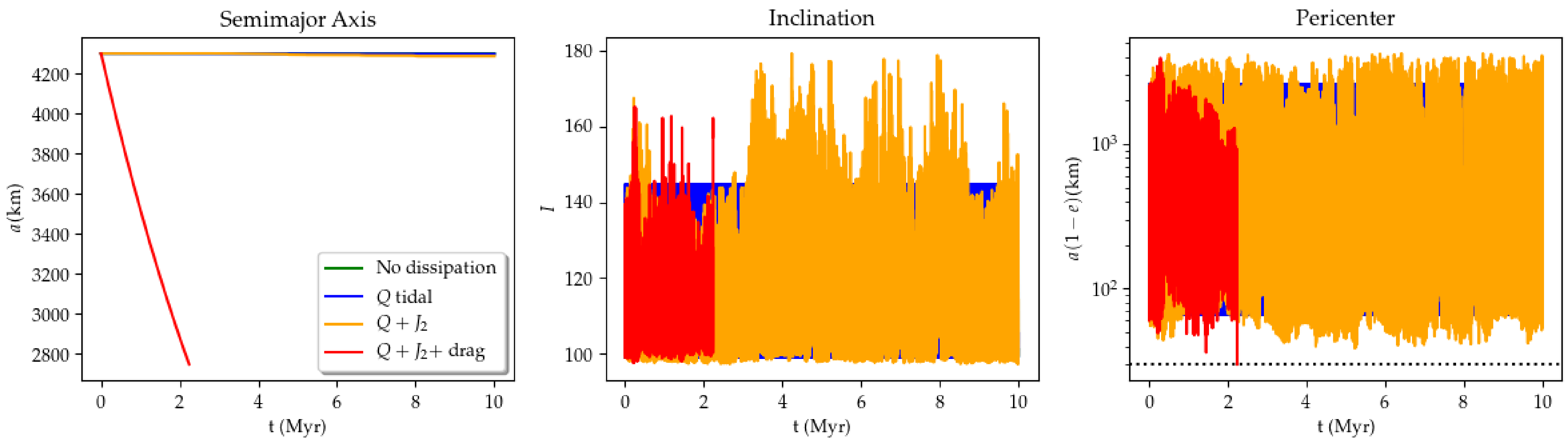

Lyra, Youdin, & Johansen (2021)

W. Lyra

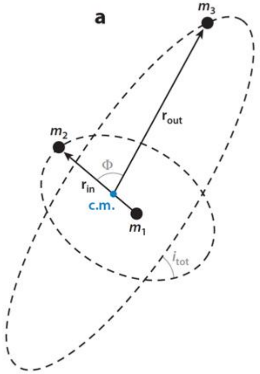

Caveat: limited by double-averaging

Double-Averaged vs Single-Averaged

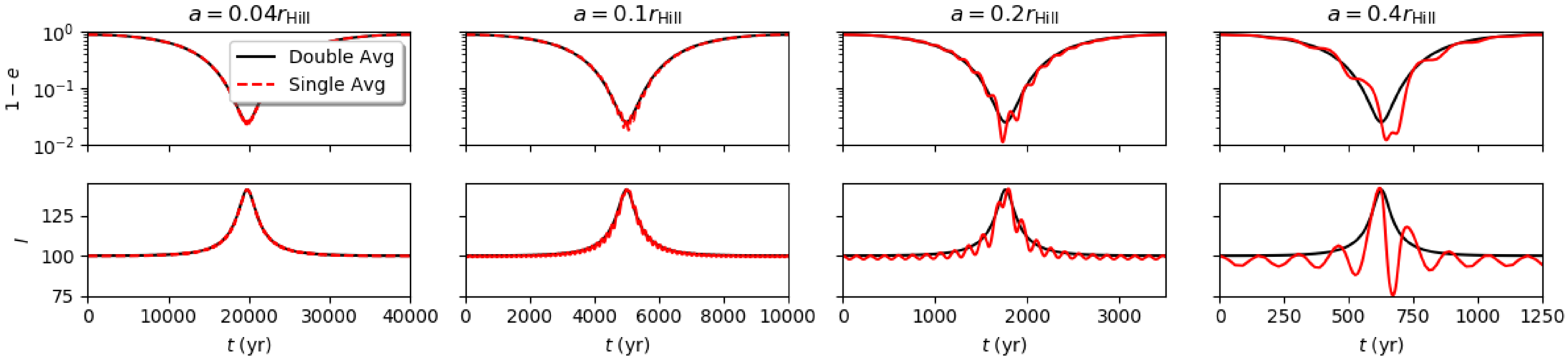

Lyra, Youdin, & Johansen (2021)

W. Lyra

Alignment of the Spin Vectors

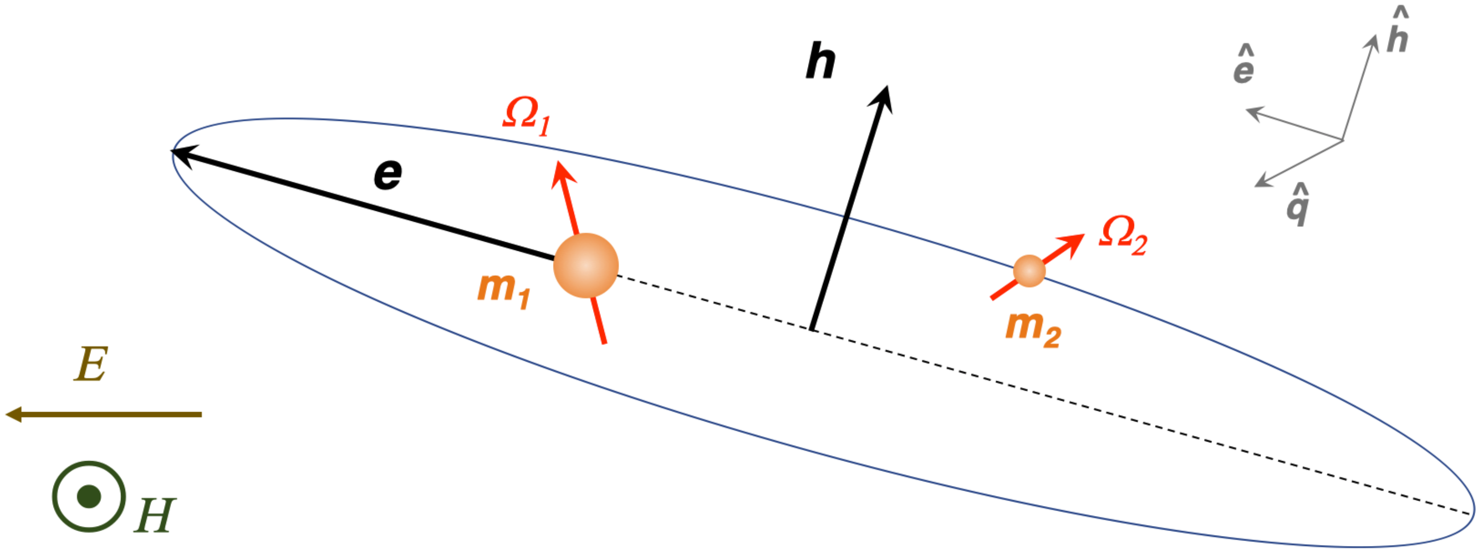

Mainly driven by J_2 (permanent quadrupole)

Timescale proportional to a^4 *(4th power of semimajor axis)*

5 Gyr for a/R ~ 100

0.5 Myr for a/R ~ 10

Lyra, Youdin, & Johansen (2021)

N-body simulations (no tides, J2, or drag)

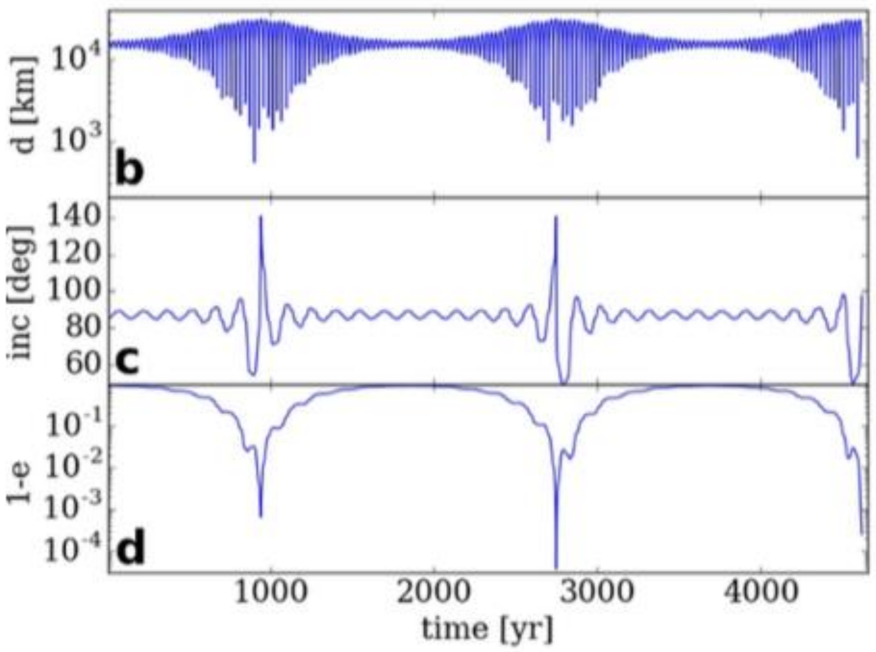

Inclination not limited to the double-averaged constraint.

Cycles lead to lower inclination than initial.

Prograde/retrograde flipping possible.

Grishin et al. (2020)

N-body simulations (no tides, J2, or drag)

Pericenter

Time to contact

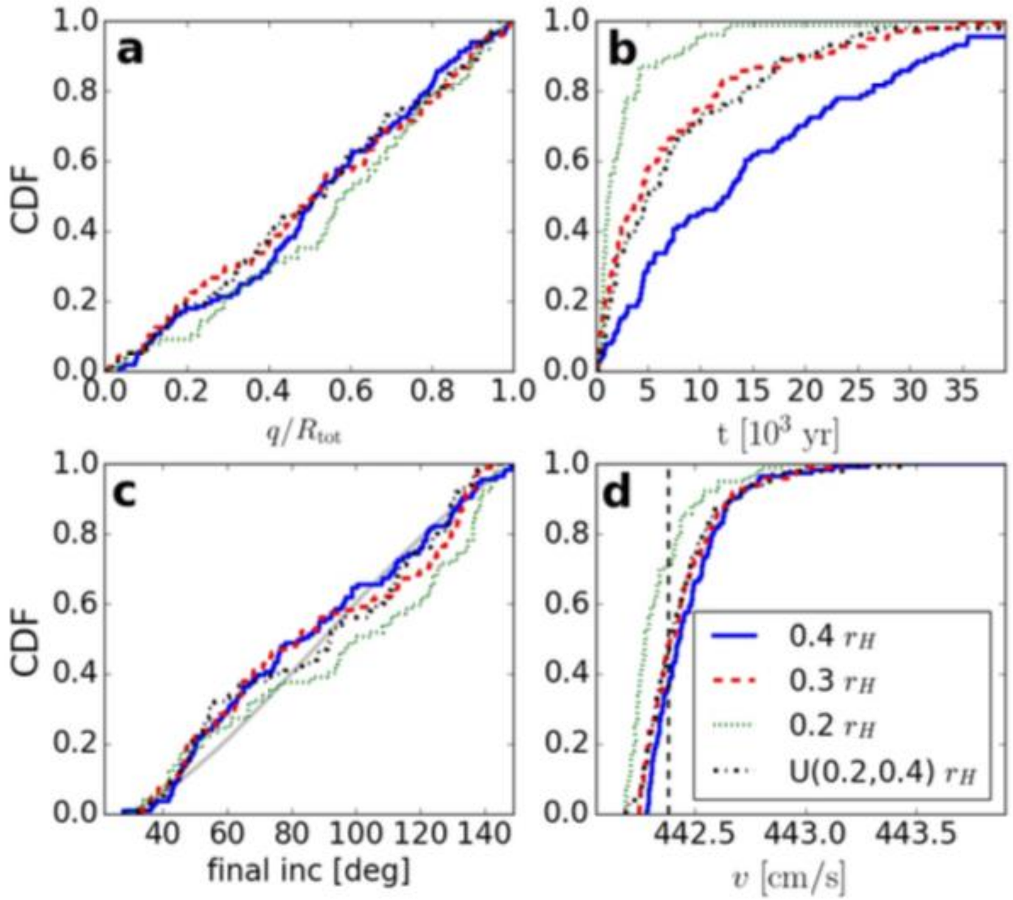

Inclination at contact

Speed at contact

Grishin et al. (2020)

N-body simulations (no tides, J2, or drag)

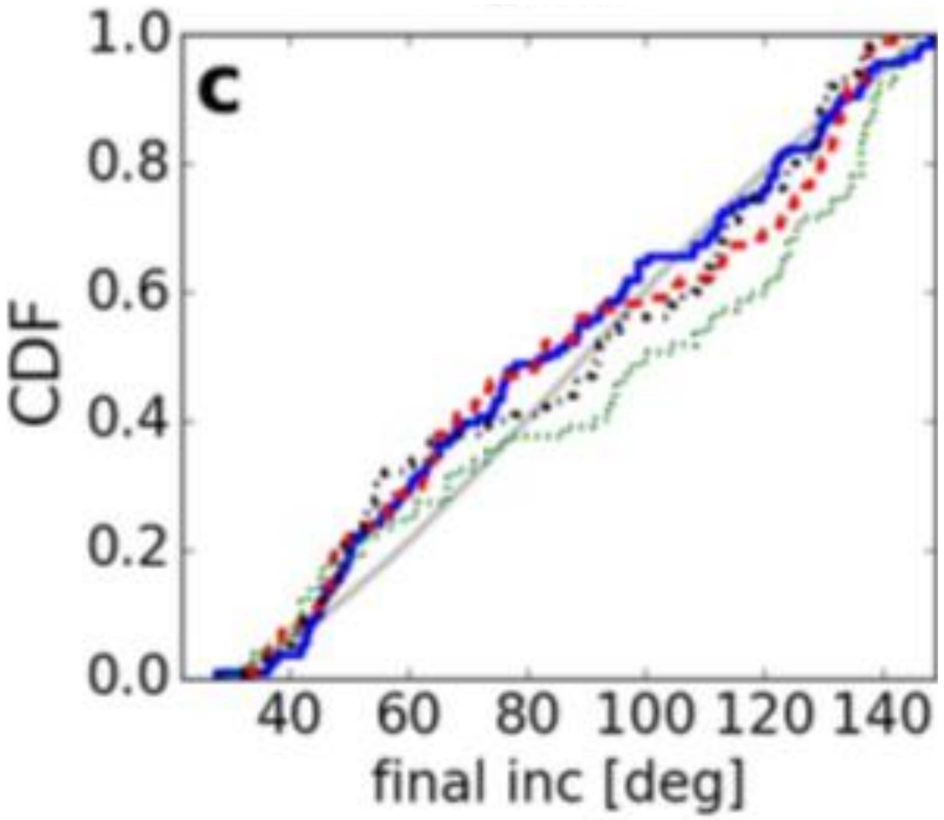

Inclination at contact

Uniform
any inclination (from 40º to 140º) equally likely

Grishin et al. (2020)

N-body simulations (no tides, J2, or drag)

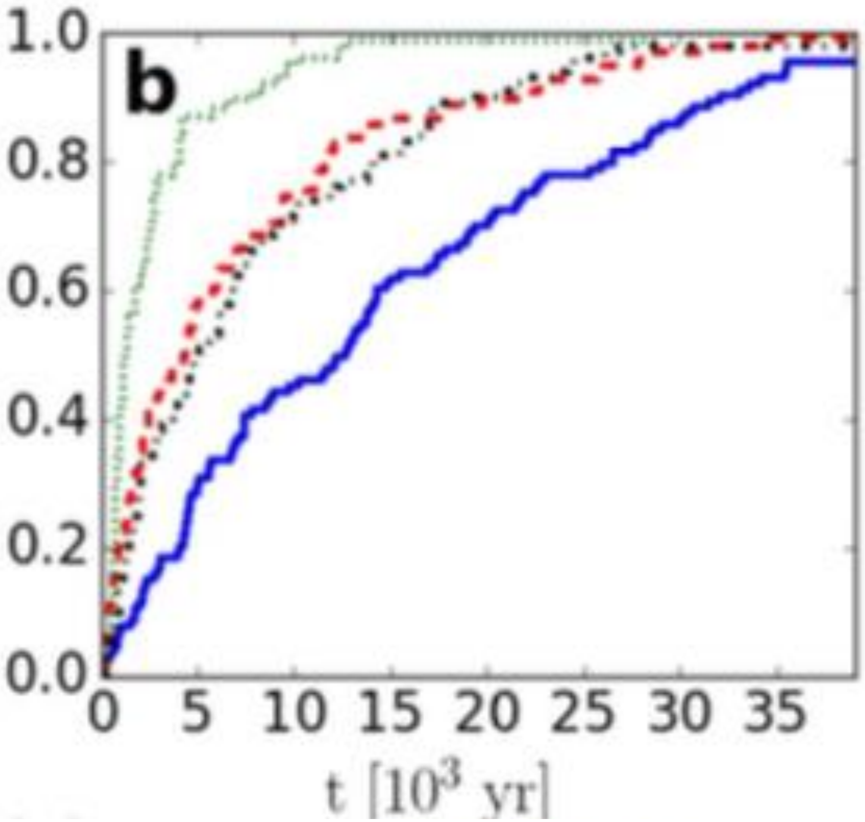

Grishin et al. (2020)

Time to contact

Too short to allow for alignment

Problem with Sky crater?

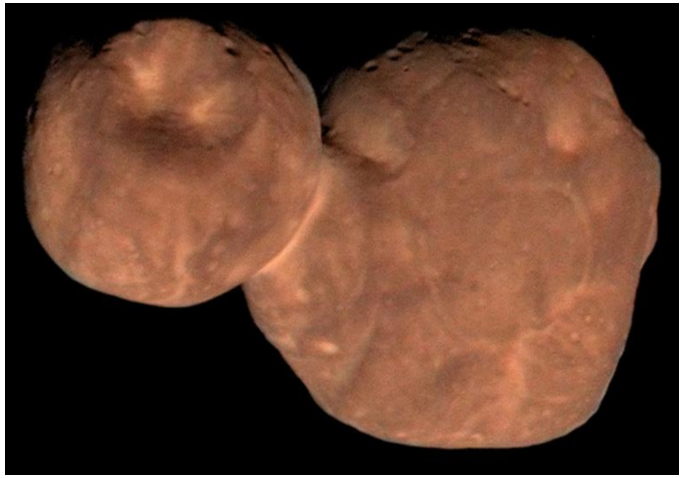

Stokes number in McKinnon et al. *1-2 Myr* vs Lyra et al. *10-20 Myr*

Traced to four different assumptions:

1) Disk model (density and temperature)
2) Viscosity
3) Drag coefficient
4) Drag time

Quantity	McKinnon et al. (2020)	Lyra, Youdin, & Johansen (2021)	Factor	Impact on τ_{drag}
Density	10^{-10} kg/m^3 (Desch et al.)	3×10^{-11} kg/m^3 (MMSN)	1.15	23 Myr -> 20 Myr
Temperature	30K	42K		
Kinematic viscosity	7×10^4 m^2/s (used sound speed)	1.4×10^5 m^2/s (used mean thermal velocity)	1.8	20 Myr -> 13 Myr
Drag coefficient C_d	$24/Re^{0.6}$	$24/Re(1+0.27)^{0.43} + 0.47[1-\exp(-0.04 Re^{0.38})]$	1.5	13 Myr -> 9 Myr
Drag time τ_{drag}	$\rho R/(C_d \rho_g u_{wind})$	$8/3 \times \rho R/(C_d \rho_g u_{wind})$	2.7	9 Myr -> 3 Myr

Conclusions

- Solved the binary planetesimal problem with gas drag
- Implemented the solution into a Kozai plus tidal friction code
- Contact possible in the asteroid belt within 0.1 Myr (depleted of binaries)
- Contact via Kozai cycles in the Kuiper belt, orbits become grazing
- Window of contact increased by J_2 and drag

- Model predictions:
  - ~ 10% of KBCC binaries should be contact binaries
  - Velocities at contact should be about 3-4 m/s

- Open questions:
  - Single-averaged (or N-body) needed to reproduce final inclinations
  - Combine our model with single-averaged Kozai (or N-body)

...1 January 2019.

The two bodies slowly spiral closer until they touch, forming the bi-lobed object we see today.

Sketch by J.T. Keane

Lyra, Youdin, & Johansen (2021)